Plant Physiology Preview. Published on July 14, 2017, as DOI:10.1104/pp.17.00375

BcXYG1, a Secreted Xyloglucanase from *Botrytis cinerea*, Triggers Both Cell Death and Plant Immune Responses

Wenjun Zhu[1,7], Mordechi Ronen[1], Yonatan Gur[1], Anna Minz-Dub[1], Gal Masrati[2], Nir Ben-Tal[2], Alon Savidor[3], Itai Sharon[1], Elad Eizner[1,4], Oliver Valerius[5], Gerhard H. Braus[5], Kyle Bowler[6], Maor Bar-Peled[6], Amir Sharon[1]

[1]Department of Molecular Biology and Ecology of Plants, Faculty of Life Sciences, Tel Aviv University, Tel Aviv 69978, Israel

[2]Department of Biochemistry and Molecular Biology, Faculty of Life Sciences, Tel Aviv University, Tel Aviv 69978, Israel

[3]Nancy and Stephen Grand Israel National Center for Personalized Medicine, Weizmann Institute of Science, Rehovot 76100, Israel

[4]Department of Physical Electronics, Fleischman Faculty of Engineering, Tel Aviv University, Tel Aviv 69978, Israel

[5]Complex Carbohydrate Research Center, CCRC; Department of Plant Biology, University of Georgia Athens, GA 30602-4712

[6]Department of Molecular Microbiology and Genetics and Göttingen Center for Molecular Biosciences (GZMB), Georg-August-Universität Göttingen, Germany

[7]College of Biology and Pharmaceutical Engineering, Wuhan Polytechnic University, Wuhan 430023, People's Republic of China

Corresponding author: Amir Sharon, Department of Molecular Biology and Ecology of Plants, Tel Aviv University, Tel Aviv 69978, Israel. amirsh@ex.tau.ac.il

Summary: A cell death-inducing apoplastic protein facilitates necrosis and establishment of the pathogen Botrytis cinerea, but is also recognized by the plant immune system and triggers a defense response

Running title: A Botrytis cell death-inducing apoplastic protein

ABSTRACT

In search of *Botrytis cinerea* cell death-inducing proteins, we found a xyloglucanase (BcXYG1), which induced strong necrosis and a resistance response in dicot plants. Expression of the *BcXYG1* gene was strongly induced during the first 12 hours post inoculation, and analysis of disease dynamics using PathTrack© showed that a *B. cinerea* strain over expressing *BcXYG1* produced early local necrosis supporting a role of BcXYG1 as an early cell death-inducing factor. The xyloglucanase activity of BcXYG1 was not necessary for induction of necrosis and plant resistance, as a mutant of BcXYG1 lacking the xyloglucanase enzymatic activity retained both functions. Residues in two exposed loops on the surface of BcXYG1 were found necessary for induction of cell death, but not for inducing plant resistance. Further analyses showed that BcXYG1 is apoplastic and possibly interacts with the proteins of plant cell membrane, and that the BcXYG1-cell death-promoting signal is mediated by the LRR receptor-like kinases BAK1 and SOBIR1. Our findings support the role of cell death-inducing proteins in establishing infection of necrotrophic pathogens and highlight the recognition of fungal apoplastic proteins by the plant immune system as an importance mechanism of resistance against this class of pathogens.

INTRODUCTION

B. cinerea is a wide-host range fungal pathogen, causing grey mold and rot diseases in a large number of agriculturally important crops, and has been used as a model system to study pathogenicity in necrotrophic plant pathogens. *B. cinerea* infection process includes two typical stages: an early stage characterized by local lesions, followed by a late stage of fast spreading lesions (Williamson et al., 2007). Recent studies of disease dynamics conducted with the aid of a PathTrack© system lead to discovery of a third, intermediate stage, between the transition from local infection to lesion spreading (Eizner et al., 2017). Further analysis using this system revealed that differences in disease progression between wild type and pathogenicity mutants were largely in parameters of the intermediate stage, highlighting it as the phase during which the fungus is most significantly exposed and affected by the plant defense. The initial phase was much less affected by fungal mutations or by external conditions, suggesting that it depends primarily on the ability of the fungus to form local necrosis. This result is in line with a previous work showing that towards the end of the early phase (about 36 hours post infection; hpi) and the beginning of the late stage (about 48 hpi), the fungus undergoes massive cell death, which is induced by the plant defense (Shlezinger et al., 2011). A working model derived from these findings proposed that during early infection phase, the fungus forms local necrosis without invading the host tissue. The model also predicts early secretion of cell death-inducing factors and fast formation of small spots of dead tissue, in

which the fungus can establish itself and use as foci for growth in the following stages (Shlezinger et al., 2011).

A relatively small number of effectors have been described in host-specific and broad host range necrotrophic pathogens, compared to the wealth of information and large number of effectors described in biotrophic and hemibiotrophic fungal pathogens. For example, Victorin from the oat pathogen *Cochliobolus victoriae* triggers HR-like resistance in *Arabidopsis thaliana*, thereby facilitating disease of necrotrophic pathogens (Lorang et al., 2007; Lorang et al., 2012). *Parastagonospora nodorum* and *Pyrenophora tritici-repentis*, two host-specific wheat pathogens, secrete multiple effectors that induce severe necrosis and confer disease susceptibility in wheat genotypes with the specific corresponding sensitivity genes (Oliver et al., 2012; Gao et al., 2015; Shi et al., 2015). Effectors described in broad host range necrotrophic fungi are primarily classified as necrosis-inducing proteins (NIPs). Proteins in this category can induce necrosis in a wide range of dicot plants, and in a few cases, were found important for infection (Frías et al., 2011; González et al., 2016; Oliver and Solomon, 2010). Main groups of NIPs are cerato platanins, and the necrosis and ethylene inducing proteins [NEP and NEP-like (NLP)]. Recent studies showed that some NIPs are recognized by the plant immune system, leading to pathogen associated molecular patterns (PAMP)-triggered immunity (PTI). For example, nlp20, a conserved 20-amino-acid fragment found in most NLPs, interacts with the *A. thaliana* leucine-rich repeat receptor protein (LRR-RP) RLP23, and the resulting immunity signal is transmitted via RLP23-SOBIR1-BAK1 complex (Albert et al., 2015).

Cell wall degrading enzymes (CWDEs) play a central role in diseases caused by necrotrophic pathogens by maceration of host tissues at late stages of the disease. These enzymes hydrolyze the glycoside bond between two or more carbohydrates or between a carbohydrate and a non-carbohydrate residue, thereby reducing complex sugar polymers to simple sugars (Cantarel et al., 2009; Kubicek et al., 2014). Some CWDEs activate the plant immune response, either directly or through the release of cell wall elicitors (Benedetti et al., 2015; Ma et al., 2015, Poinssot et al., 2003; Wu et al., 2016; Zhang et al., 2014b), and may also induce necrosis when injected to plant tissues (Ma et al., 2015; Noda et al., 2010; Zhang et al., 2015; Zhang et al., 2014b). In certain cases, this necrosis inducing activity was found to be unrelated to the enzymatic activity, thus defining another class of NIPs. For example, Xyn11A, a *B. cinerea* glycosyl hydrolase family 11 xylanase, induces cell death in plant leaves independent of the xylanase activity, and is necessary for full virulence of *B. cinerea* (Brito et al., 2006; Noda et al., 2010). The *Trichoderma viride* ethylene inducing xylanase (EIX), another glycosyl hydrolase family 11 xylanase, induces necrosis in tobacco and tomato leaves independent of the enzymatic activity (Furman-Matarasso et al., 1999). XEG1

produced by the soybean pathogen *Phytophthora sojae* triggers cell death and plant defense responses in a BAK1-dependent manner and independent of its xyloglucanase activity (Ma et al., 2015).

Recent findings have demonstrated that the plant apoplast is most likely a battleground where a variety of plant–pathogen interactions occur and determine the outcome of pathogen infections (De Wit, 2016; Du et al., 2016). Accordingly, and based on our working model (Shlezinger et al., 2011), we anticipate secretion of NIPs to the plant apoplast by *B. cinerea* in early infection stages. In search of such cell death-inducing virulence proteins, we conducted a proteomic analysis of *B. cinerea* secretome that was collected from infected leaves and screened candidates for necrosis-inducing activity. Here, we report on the identification and characterization of BcXYG1, a secreted GH12 xyloglucanase and an apoplastic protein with strong necrosis-inducing activity. We show that the BcXYG1 death-inducing signal is mediated by the plant LRR receptor-like kinases BAK1 and SOBIR1, that in addition to induction of cell death, BcXYG1 is recognized by the plant immune system and activates defense responses, and that the enzymatic activity is not necessary for induction of either cell death or plant defense responses.

RESULTS

B. cinerea Secretome Contains Necrosis-Inducing Proteins

Fungal effectors and virulence proteins are specifically expressed during the infection stages in which they play a role. We therefore developed a system to collect fungal secretome from inoculated plants, expecting it to be enriched for *in planta*-expressed plant-affecting proteins. According to our *B. cinerea* infection model, we expect that it uses necrosis inducing molecules at the early infection stage (Shlezinger et al., 2011). We therefore anticipated necrosis-inducing activity in the fungal secretome collected from leaves rather early after inoculation, and indeed, the purified *B. cinerea* secretome caused necrosis in *N. benthamiana* leaves as early as 22 hpi (Fig. 1A), coinciding with a steep increase in the amount of secreted proteins (Fig. 1B). Based on the activity and protein amounts, we selected the 28 hpi time point for all further analyses. When the fungus was grown on a glass slide for the same period of time it developed comparable amounts of mycelia, however necrosis-inducing activity of the secretome from glass-grown fungus was much weaker (Fig. 1C), supporting enrichment of the leaf-collected secretome with necrosis-inducing factors. In addition to *N. benthamiana*, the secretome caused necrosis in all other plant species that we examined, including maize and wheat (data not shown). Induction of necrosis was lost when the

secretome was boiled or when proteins were precipitated with ammonium sulfate [$(NH_4)_2SO_4$], and retained within the tubes following ultrafiltration through 10 kDa (Fig. 1D), confirming that the necrosis is induced by secreted proteins.

Proteomic Analysis of the Secretome

A total of 259 secreted proteins were identified in the secretome of the wild type strain (Supplemental Table S3). The largest groups included enzymes of carbohydrate hydrolysis, proteins of unknown function, cell wall degrading enzymes, oxidoreductase, and proteases (Supplemental Fig. S1). Besides minor differences in percentages, the overall partitioning of the proteins among functional categories was similar to previously reported analyses of *B. cinerea* secretome (González et al., 2016). To identify potential NIPs, we compared the wild type secretomes and two pathogenicity mutants: 1) Δ*bcnoxA*, which has a deletion of the NADPH oxidase catalytic subunit. This strain is able to penetrate host tissue in the same way as the wild type, but shows much slower spreading and plant colonization (Segmüller et al., 2008). 2) CA-BcRAC, a strain expressing a constitutively active (CA) allele of the small GTPase BcRAC, which causes earlier and more intense necrosis than the wild type (Minz-Dub et al., 2013). Comparing the presence and abundance of proteins among the different strains (Supplemental Tables S4 and S5) allowed us to exclude certain proteins and to categorize others as high or low priority. Additional criteria used to prioritize candidate proteins were peptide abundance, presence of a secretion signal, predicted function, and molecular weight of the protein (≤600 amino acid). The first 20 proteins in the priority list were screed by Agrobacterium infiltration assay of *N. benthamiana* leaves (Supplemental Tables S6), and among them we found BC1G_00594, which showed strong necrosis inducing activity and was further characterized.

BC1G_00594 Is a Glycoside Hydrolase Family 12 (GH12) Protein

The *B. cinerea BC1G_00594* is a single copy gene, consisting of four exons and three introns. The first 18 N terminal amino acids encode a signal peptide and the entire predicted protein includes 248 amino acids with two cysteine residues (C^{33} and C^{61}). No transmembrane helices of this protein were predicted using *TMHMM Server v. 2.0* (http://www.cbs.dtu.dk/services/TMHMM/), indicating that the protein encoded by *BC1G_00594* is secreted, as is also evident from its presence in the *B. cinerea* secretome. BLAST searches of fungal genomes with BC1G_00594 showed the presence of homologs in a large number of necrotrophic and hemibiotrophic plant pathogens, as well as in saprotrophic fungal species, but we could not find homologues of the protein in biotrophic plant pathogens including *Blumeria graminis* f. sp. *hordei*, *Ustilago maydis* and *Puccinia* spp., or in the human pathogen *Candida albicans*. Multiple sequence alignment and phylogenetic analysis revealed significant sequence conservation (Supplemental Figs.

S2, A and B), especially of the two cysteine residues, which are well conserved in all of the BC1G_00594 homologs (Supplemental Fig. S2A). These cysteine residues are possibly involved in the formation of disulfide bonds (Sevier and Kaiser, 2002) and therefore might play a significant role in the structure and function of the protein. Prediction of the 3D structure of the BC1G_00594 protein using I-TASSER showed that it shares strong structural similarity with XEG1, a GH12 protein (XP_009525815.1) from *P. sojae* that is important for virulence (Ma et al., 2015). BLAST search of the *B. cinerea* genome in the *JGI* database uncovered another GH12 protein (BC1G_01008) with relatively low similarity to BC1G_00594 and other necrosis-inducing GH12 proteins (Supplemental Fig. S3). We named the BC1G_00594 protein "BcXYG1", as this is the first report of *B. cinerea* Xyloglucanase, and the BC1G_01008 protein "BcXYG2".

BcXYG1 Induces Cell Death in Dicot Plants

We examined the necrosis-inducing activity of BcXYG1 in plants other than *N. benthamiana.* To avoid possible effects on protein production by *A. tumefaciens* compatibility, BcXYG1 was produced in *E. coli* (Fig. 2A), and the purified protein was infiltrated to leaves' mesophyll using a syringe. Treatment of *N. benthamiana* leaves with BcXYG1 concentrations ranging from 10 μg/ml to 200 μg/ml resulted in strong necrosis at all of the tested concentrations (Fig. 2B), unlike either EGFP or BcXYG2, which had no effect even at 100 μg/ml (Fig. 2C). Similar results were obtained with additional dicot plants, including tomato and beans, but not in monocot plants, including maize and wheat (Fig. 2D). Hence, BcXYG1 has a strong necrosis-inducing activity in dicot plants, but similar to other *B. cinerea* NIPs, it does not promote necrosis in cereals (Fig. 2D).

Induction of Necrosis Is Independent of the Glycosyl Hydrolase Activity of BcXYG1

In *Trichoderma reesei* GH12 protein, two highly conserved catalytic residues E^{116} and E^{200} are essential for the xyloglucan hydrolyzing activity (Sandgren et al., 2005). The corresponding catalytic residues in *B. cinerea* BcXYG1 are E^{142} and E^{229} (Supplemental Fig. S2A). In addition, certain CWDEs can trigger plant cell death, and in a few cases the enzymatic activity was found to be unrelated to the cell death inducing activity (Furman-Matarasso et al., 1999; Ma et al., 2015; Noda et al., 2010; Poinssot et al., 2003; Zhang et al., 2014b). To determine if the hydrolase activity of BcXYG1 is necessary for induction of necrosis, we mutated E^{142} and E^{229} to glutamine using site directed mutagenesis. Enzymatic assays with purified mutated protein (MBcXYG1) showed complete loss of the xyloglucan-degrading endoglucanase activity (Supplemental Fig. S4A). Infiltration of *N. benthamiana* with purified mutant protein (Fig. 2C), or Agrobacterium-infiltration assay (Supplemental Fig. S4B), both showed that the MBcXYG1 mutant protein retained full necrosis-inducing activity. Infiltration of leaves with purified MBcXYG1 protein also induced cell death in additional dicot plants, but not in wheat and maize, similar to the effects of wild type

BcXYG1 (Fig. 2D). These results confirm the xyloglucanase activity of BcXYG1, and show that it is not necessary for induction of plant cell death by BcXYG1.

BcXYG1 is Active Outside of the Plant Cell

To verify secretion of BcXYG1, we generated *B. cinerea* strains over expressing *BcXYG1-HA*, cultured them in PDB liquid medium, and checked for the presence of the protein in the culture filtrate. Western blot analysis confirmed accumulation of the BcXYG1-HA fusion protein in the culture medium (Fig. 3A), providing conclusive proof that BcXYG1 is secreted by the fungus. To determine if BcXYG1 triggers cell death by interaction with extracellular or intracellular targets, we constructed *A. tumefaciens* strains expressing BcXYG1 with and without secretion signal. Two constructs were produced: 1) the N-terminal signal peptide of BcXYG1 was replaced with *A. thaliana* PR3 signal peptide (TAIR ID: AT3G12500) to produce PR3 SP-BcXYG1$^{19\text{-}248}$-HA; 2) the signal peptide was deleted to produce ATG-BcXYG1$^{19\text{-}248}$-HA. PR3 SP-Nep1$^{21\text{-}246}$-HA fusion was used as a positive control, and PR3 SP-BcXYG2$^{23\text{-}398}$-HA (homologue of BcXYG1 that does not induce necrosis) fusion protein was used as a negative control (Fig. 3, B and D). Immunoblot analysis confirmed that all the examined proteins were expressed in *N. benthamiana* following Agrobacterium-mediated transient expression (Fig. 3C). Plants treated with *A. tumefaciens* expressing either PR3 SP-BcXYG1$^{19\text{-}248}$-HA or PR3 SP-Nep1$^{21\text{-}246}$-HA fusion proteins, both of which are secreted from the plant cells to the apoplast, developed the typical necrosis, whereas expression of ATG-BcXYG1$^{19\text{-}248}$-HA, which lacks the signal peptide and is therefore remains inside the cell, did not trigger cell death (Fig. 3D). These results indicate that BcXYG1 triggers cell death by interacting with extracellular components, either in the cell wall or the cell membrane.

BcXYG1 Does Not Affect Fungal Growth, Colony Morphology and Stress Tolerance

To determine the possible effects of *BcXYG1* on fungal development and pathogenicity, we generated *BcXYG1* deletion strains (Δ*xyg1*-1 and Δ*xyg1*-2), and strains that over-express either the native protein (OEXYG1) or the enzymatic activity mutant protein (OEMXYG1), and characterized their phenotype. Deletion and over expression of the gene and protein were confirmed by PCR, and qRT-PCR, and by Western blot analyses, respectively (Fig. 3A; Supplemental Fig. S5). No differences in colony morphology and growth rate on PDA were identified in any of the mutant strains, as compared to wild type cultures (Supplemental Fig. S6, A and B). In addition, there was no difference between the mutants and the wild type control in sensitivity to different types of stresses, including salt stress (1 M NaCl), osmotic stress (1 M Sorbitol) and cell wall stress (0.3 mg/ml CFW, 0.02% SDS and 0.5 mg/ml CR) (data not shown). Native, but not heat-denatured, secretome of the wild type and Δ*xyg1* strains, had similar necrosis-inducing activity in tobacco and maize leaves (Supplemental Fig. S6C), indicating that other NIPs can compensate for the loss of

BcXYG1.

BcXYG1 is Highly Expressed at the Early Infection Stage

Transcript levels of *BcXYG1* rapidly increased following inoculation of leaves, and reached a peak of about 40-fold compared to 0 hpi at 12 hpi. The transcript levels then dropped sharply, to a level that was slightly higher than the initial level (Fig. 4). When *B. cinerea* was grown on solid Gamborg's B5 medium, expression levels of *BcXYG1* remained stable until 12 hpi, and then gradually increased reaching a maximum of about 12 fold increase compared to 0 hpi at 48 hpi (Fig. 4). The expression pattern of *BcXYG2* also rapidly increased following inoculation of leaves and peaked around 36 hpi, but it increased only about 9 fold, compared to a 40 fold increase of *BcXYG1*. On solid medium, the expression level of *BcXYG2* started to increase around 12 hpi, reaching a similar level to its expression levels on plants around 60 hpi. The early and high induction of *BcXYG1*, but not *BcXYG2*, on plants, support a role of BcXYG1 in pathogenicity of *B. cinerea*, possibly as a factor that is necessary for establishment of primary lesions during the early infection stage.

BcXYG1 contributes to production of local necrosis during early fungal establishment

According to our working model, NIPs facilitate production of local necrosis during the early stage of infection. The early expression of *bcxyg1* in *planta* further supports a role of the protein in generation of local necrosis, which is used for establishment of the infection court. To compare the pathogenicity of the wild type and *bcxyg1* transgenic strains, beans leaves were inoculated with spores of the different strains and lesion size was measured 72 hpi. A slightly larger lesion was produced by the over expression strains, however the differences were statistically insignificant (Supplemental Fig. S7), suggesting that deletion or over expression of *BcXYG1* does not affect final outcome of infection. To gain insight into possible unnoticed effects caused by BcXYG1, particularly during the early infection stage, we characterized infection of the *bcxyg1* over expression and deletion strains using the PathTrack© system. This system allows for sensitive and quantitative analysis of infection dynamics, and therefore can reveal small changes in disease development (Eizner et al., 2017). The pathogenic behavior of the Δ*bcxyg1* deletion strain was similar to that of the wild type in all of the examined parameters, including time and magnitude of early necrosis, break time and lesion expansion rate (Fig. 5). This result might not be surprising considering that the secretome contains additional NIPs that can compensate for the lack of BcXYG1 (as shown in Supplemental Fig. S6C). The OEXYG1 (over expression of native BcXYG1) and OEMXYG1 (over expression of BcXYG1 that lacks enzymatic activity) strains, both produced significantly earlier and more intense local necrosis, and had a slightly earlier, but statistically insignificant, break time than the wild type strain (Fig. 5). All of the examined strains, including the

wild type, the deletion and the different over expression strains had similar lesion expansion rate, which can explain the similar final lesion size at 72 hpi.

BcXYG1 Triggers PTI and Induces Systemic Resistance in Bean

Recent reports showed that at least some necrosis inducing proteins are recognized by the plant immune system and can activate PTI (Frías et al., 2016; Zhang et al., 2014b). To assess whether BcXYG1 could induce resistance in addition to cell death, one of two primary bean leaves was infiltrated with 100 μg/ml of either BcXYG1 or MBcXYG1, and after two days the second, untreated leaf, was inoculated with *B. cinerea*. In plants that were pre-infiltrated with BcXYG1 or MBcXYG1, lesion size on the infected leaf was significantly smaller compared to lesions size on leaves in untreated plants or plants that were pre-infiltrated with BcXYG2 or EGFP (Fig. 6A). RT-PCR analysis of gene expression in untreated leaves showed marked increase of the plant defense genes *Pvd1* (GenBank: HM240258.1), *PvPR1* (GenBank: CAA43637.1) and *PvPR2* (GenBank: CAA43636.1) following infiltration of the other leaf with BcXYG1 or MBcXYG1, compared to a modest increase in plants that were pretreated with either BcXYG2, EGFP, or blank (Fig. 6B). These results show that BcXYG1 induces systemic resistance in bean plants, which is independent of its xyloglucanase activity. Interestingly, although BcXYG1 and MBcXYG1 both induced similar levels of necrosis and triggered systemic resistance, the expression levels of defense genes in BcXYG1-pretreated plants were significantly higher than in MBcXYG1-pretreated plants (Fig. 6B). This result suggests that the xyloglucan hydrolysis products produced by BcXYG1 also contribute to induction of plant defense.

Necrosis-Inducing Activity of MBcXYG1 is Dependent on Its Tertiary Structure

Previous study demonstrated that certain plant cell wall residues such as oligogalacturonides and oligosaccharides that are released by enzymatic hydrolysis could activate plant defense responses (Benedetti et al., 2015; Ferrari et al., 2013; Trouvelot et al., 2014; Wu et al., 2016). To eliminate the possible effect of xyloglucans hydrolysis products on plant systemic resistance, we used xyloglucanase activity mutant MBcXYG1 for subsequent studies.

Denaturation of BcXYG1 by incubation at 95°C for 15 minutes abolished the necrosis-inducing activity (Fig. 7A), indicating that the tertiary structure of BcXYG1 is important for this function. Structural analysis of BcXYG1 using *PredictProtein* (https://www.predictprotein.org/) predicted formation of an intramolecular disulfide bond by cysteine residues C^{33} and C^{61} (Supplemental Fig. S2A), that are essential for protein folding and for maintenance of the tertiary structure (Marianayagam et al., 2004; Sevier and Kaiser, 2002). To verify if necrosis-inducing activity of BcXYG1 depends on its intact tertiary structure, we replaced MBcXYG1 C^{33} and C^{61} with alanine, either individually or simultaneously. In addition, we deleted the last 12 amino acids

(VFKTTAYSVSLN, 237-248 amino acid) of the protein, which constitute a β-strand that is important for maintaining the structural integrity and stability of BcXYG1 (Fig. 7D). All of the examined mutations resulted in complete loss of the necrosis-inducing activity of the protein, as demonstrated by Agrobacterium-infiltration assay of *N. benthamiana* (Fig. 7, B-F). Hence, disruption of the tertiary structure destroys the necrosis-inducing activity of BcXYG1.

Previous studies reported that two surface-exposed loops comprise a conserved two-peptide motifs on the surface of elicitor BcSpl1. The two motifs interact with each other to form a small protrusion on the protein surface and contribute synergistically to triggering of necrosis (Frías et al., 2014), indicating that proper space distance and position of the active epitope motifs are important for the necrosis-inducing activity of this protein (Frías et al., 2014). Analysis of surface accessibility of BcXYG1 using *ASA-View* (http://www.abren.net/asaview/) showed that the peptides GSN (118-120 amino acid) and SETGS (157-161 amino acid) are surface-exposed (Supplemental Fig. S8), and constitute two protrusive loop structures on the surface of the protein (Supplemental Fig. S3C). In addition, these two short stretches are not conserved in BcXYG2 (Supplemental Fig. S3A), implying that either or both of the peptides $GSN^{118-120}$ and $SETGS^{157-161}$ might be important for the necrosis-inducing activity of BcXYG1. To verify this possibility, we replaced the residues $GSN^{118-120}$ with $AAA^{118-120}$, and the residues $SETGS^{157-161}$ with $AAAAA^{157-161}$, individually or simultaneously, and transiently expressed the mutant proteins in *N. benthamiana* leaves using Agrobacterium-infiltration. Neither the $GSN^{118-120}$ or the $SETGS^{157-161}$ mutations alone had an effect on the necrosis-inducing activity of the protein, but simultaneous mutation of both sites completely abolished it (Fig. 8, A and B). Furthermore, simultaneous mutations of two other pairs of surface-exposed peptides, $TGSY^{41-44}$ and $TSNS^{68-71}$, and $WNITG^{51-55}$ and $GGSSQ^{82-86}$, did not affect necrosis-inducing activity (Fig. 8, A and B). Hence, both the $GSN^{118-120}$ and $SETGS^{157-161}$ motifs are necessary for induction of necrosis by BcXYG1, and each of them alone is sufficient for full necrosis-inducing activity. Integration of the $GSN^{118-120}$ and $SETGS^{157-161}$ motifs into BcXYG2 did not confer necrosis-inducing activity in this protein (Fig. 8, C-E), suggesting that additional properties such as proper space distance and position of the active epitope motifs, are critical for the necrosis–inducing activity, as was found in the NIP BcSpl1 (Frías et al., 2014).

Defense Stimulation by BcXYG1 is Unrelated to Necrosis-Inducing Activity

We used the $GSN^{118-120}$ / $SETGS^{157-161}$ mutant protein to test if necrosis is necessary for induced plant defense. Bean leaves were infiltrated with the $MBcXYG1^{(GSN118-120AAA\ SETGS157-161AAAAA)}$ protein and the other leaf was inoculated with *B. cinerea* as described above. The $MBcXYG1^{(GSN118-120AAA\ SETGS157-161AAAAA)}$ protein induced systemic resistance similar to that induced by MBcXYG1, as determined by lesion size and expression of defense genes (Fig. 9, A and

B). Hence, abolishment of necrosis-inducing activity did not abolish activation of the plant defense system by BcXYG1, suggesting that the plant immune response is triggered by recognition of BcXYG1 and not the necrosis that is cause. To verify this possibility, we tested the effect of Dukatalon (132 g/L Praquat, 66 g/L Diquat), a herbicide that induces necrosis, on activation of plant resistance. Treatment with Dukatalon caused strong cell death in bean leaves, but it did not affect lesion size on the second leaf (Supplemental Fig. S9), indicating that induction of necrosis is not the cause of defense activation. Additional experiments showed that activation of the plant defense is lost if the protein is denatured (by boiling) or destabilized (by peptide deletion) (Supplemental Fig. S10). We therefore concluded that similar to necrosis induction, intact tertiary structure of BcXYG1 is necessary for activation of the plant defense, but the cell death and defense-stimulating activities are probably mediated by different epitopes.

BcXYG1 is Targeted to Plant Membrane and Its Activity Is Mediated by BAK1 and SOBIR1

As demonstrated above, BcXYG1 needs to be in the plant extracellular space to induce cell death (Fig. 3D). To determine the site of action of BcXYG1 as either the plant cell wall or the cell membrane, tobacco protoplasts were incubated with 100 μg/ml of either MBcXYG1 (induces full necrosis) or MBcXYG1$^{(GSN118\text{-}120AAA\ SETGS157\text{-}161AAAAA)}$ (does not induce necrosis), and the number of intact protoplasts was counted. When incubated with MBcXYG1, the number of intact protoplasts rapidly decreased compared to protoplasts that were incubated with either MBcXYG1$^{(GSN118\text{-}120AAA\ SETGS157\text{-}161AAAAA)}$ or PBS (Fig. 10A). Within 1 h of incubation with MBcXYG1, protoplasts showed chloroplast disorganization and cell shrinkage, and eventually disintegrated (Fig. 10B). This result shows that BcXYG1 does not need the cell wall for affecting cells, and hence it probably targets the plasma membrane.

Many fungal effectors interact with plant receptor-like proteins (RLPs), which transmit the signals via the LRR receptor-like kinases SOBIR1 and BAK1 (Albert et al., 2015; Liebrand et al., 2013; Postma et al., 2016; Zhang et al., 2014b; Zhang et al., 2013). Because BcXYG1 probably induces cell death through interaction with the plant cell membrane, it is possible that it is recognized by a membrane RLP, and that the signal is mediated by a RLP-SOBIR-BAK1 complex. To address this possibility, we used VIGS to induce gene silencing of *NbBAK1* or *NbSOBIR1* in *N. benthamiana* leaves. When infiltrated with MBcXYG1, the *NbBAK1*- or *NbSOBIR1*-silenced plants developed delayed symptoms and the majority of the spots were either unaffected or developed late chlorosis (Fig. 11). Mature necrotic spots were observed in only 28.57% and 46.15% of the *NbBAK1*- and *NbSOBIR1*-silenced leaves, respectively, compared with 100% necrotic spots in control plants or plants that were infiltrated with a pTRV2-*GFP*. Interestingly, the *NbBAK1*-silenced leaves always showed a lower level of necrosis than the *NbSOBIR1*-silenced leaves. These

results show that SOBIR1 and BAK1 mediate the necrosis-inducing activity of BcXYG1, possibly through an upstream RLP.

DISCUSSION

Upon first contact with a plant, necrotrophic pathogens face a dilemma: they have a limited capacity to extract nutrients from living tissues, yet they need to survive in a hostile live environment. Several reports have suggested that the solution might be a brief "biotrophic" phase that precedes killing of plant cells and allows fungi such as *B. cinerea* and *Sclerotinia sclerotiorum* to subvert the host defenses and establish an initial infection court (Kabbage et al., 2013; Kabbage et al., 2015; van Kan et al., 2014; Williamson et al., 2011). In our system, upon inoculation of leaves with *B. cinerea*, the spores germinate within a few hours and produce healthy and fully viable hyphae on the surface of the leaf within the first 24 hpi. Local micro lesions then appear, concomitant with attempts of the fungus to penetrate into the tissue, followed by massive fungal cell death as a result of exposure of the fungal cells to the plant defense (Shlezinger et al., 2011). We therefore predicted that the initial infection stage of *B. cinerea* is mediated by cell death promoting factors that the fungus delivers to the plant apoplast, which by instant killing of plant cell produce patches of dead tissue in which fungus is protected from the host defense and can used as initial infection courts. Here we described the identification and analysis of BcXYG1, a plant cell death-promoting apoplastic effector found in *B. cinerea* secretome collected from inoculated leaves 28 hpi. Initial tests with purified BcXYG1 showed that the necrosis-inducing activity of the protein is at least as strong as that of BcNEP1. Similar to BcNEP1 and other NIPs, the induction of necrosis by BcXYG1 is restricted to dicot plants while the entire secretome could induce necrosis in both dicot and monocot plants, suggesting the presence of different classes of NIPs in the fungal secretome.

BcXYG1 is a CWDE xyloglucanase with a glycoside hydrolase family 12 (GH12) domain (Pfam ID: PF01670). CWDEs are the largest class of *B. cinerea* secreted proteins, and many of the CWDEs found in our study, including BcXYG1, were also reported in pervious proteomic analyses (Espino et al., 2010; González et al., 2016). In our work, we collected the secretome directly from leaves, at a rather early time point (28 hpi) when, as we verified, the secretome has strong necrosis-inducing activity. Secretome from a fungus cultured on a glass slide had a significantly reduced necrosis-inducing activity compared to secretome from inoculated leaves, supporting enhanced production of NIPs *in planta*. To assist in identification of potentially important proteins present in the entire secretome, we compared secretomes from wild type and pathogenicity mutants affected at different stages of infection. This approach allowed us to identify BcXYG1 as a potential NIP based on relative high abundance in wild type secretome and a further >4-fold increase in secretome from

a CA-BcRAC strain, which causes early and more intense necrosis (Minz-Dub et al., 2013). As could be expected, we also found high levels of previously identified NIPs in the secretome (Supplemental Table S3), including NPP1 (BC1G_10306), BcSpl1 (BC1G_02163), Xyn11A (B0510_640), BcGs1 (BC1G_04151), BcIEB1 (BC1G_12374), BcPG1 (BC1G_11143), BcPG2 (BC1G_02003) and BcPG3 (BC1G_04246) (Cuesta Arenas et al., 2010; Frías et al., 2011; Frías et al., 2016; Noda et al., 2010; Zhang et al., 2015; Zhang et al., 2014b). Interestingly, in the secretome collected from the CA-BcRAC strain we also found high abundance of the NIPs NPP1 and BcSpl1 (Supplemental Table S5), which can explain the enhanced necrosis produced by this strain.

Taking several approaches, we showed that BcXYG1 is localized to the plant apoplast and that it targets the plant cell membrane (Figs. 3D and 10). Apoplastic effectors that induce cell death have been recently reported in several systems, such as *Ustilaginoidea virens* and *Zymoseptoria tritici* (Fang et al., 2016; Kettles et al., 2017). Although BcXYG1 is a xyloglucanase, we showed that induction of cell death by BcXYG1 does not require the xyloglucan degrading activity, suggesting that the cell death-inducing activity is mediated by a specific protein domain or motif. Treatment of protoplasts with a protein that lacks enzymatic activity (MBcXYG1) resulted in fast deterioration and death of the protoplasts, suggesting that recognition of BcXYG1 occurs on the cell membrane, and may be mediated by a RLP. Silencing of *BAK1* and *SOBIR1* blocked development of necrosis (Fig. 11), supporting the possibility that a RLP-SOBIR1-BAK1 complex mediates the cell death inducing activity of BcXYG1.

Studies of various NIPs showed that small epitopes located on the surface of the proteins are sufficient to induce necrosis, independent of the tertiary structure of entire protein. For example, a 30-amino acids peptide on the surface of Xyn11A mediates binding to plant cell membrane and induction of cell death (Noda et al., 2010). Similarly, a 35-amino acids peptide derived from a conserved region of BcIEB1 is sufficient for triggering necrosis as well as for PTI (Frías et al., 2016). Heat-denatured *S. sclerotiorum* SsCut could still induce necrosis in tobacco leaves and the entire C-terminal-half of the protein was found indispensable for both enzymatic and elicitor activities (Zhang et al., 2014a). Denaturation of the polygalacturonase BcPG3 did not abolish necrosis-inducing activity of this enzyme (Zhang et al., 2014b). In contrast to these examples, denaturation of BcXYG1 completely abolished both induction of necrosis and defense-stimulating activities (Supplemental Fig. S10). Therefore, unlike many other studied NIPs, the tertiary structure of BcXYG1 is vital for induction of both necrosis and PTI. In case of the necrosis-inducing activity, intact tertiary structure of BcXYG1 is necessary to allow two loop domains [GSN (118-120 amino acid) and SETGS (157-161 amino acid)] to interact with each other on the surface of the protein. A similar situation was reported for the NIP BcSpl1, where two peptide motifs interact with each other

to form a small protrusion on the protein surface, thereby synergistically contributing to induction of necrosis (Frías et al., 2014). We have not identified a domain that mediates BcXYG1-activated PTI, and therefore it is unclear whether there is a specific domain or the entire protein is necessary for this activity.

Heat treatment or structural mutation of the *Pectobacterium carotovorum* pv. *carotovorum*-derived NIP PccNLP abolished induction of necrosis as well as activation of plant defense by this effector (Böhm et al., 2014; Ottmann et al., 2009). In contrast, heat treatment or structural mutation of *P. parasitica* PpNLP, a homolog of PccNLP, abolished induction of necrosis but not of the plant defense (Böhm et al., 2014). *Hyaloperonospora arabidopsidis* HaNLP3, a NLP that lacks necrosis-inducing activity, acts as a potent activator of the plant immune system in *A. thaliana* (Oome et al., 2014). Similarly, we found that induction of cell death and plant defense by BcXYG1 are separable as demonstrated by the MBcXYG1$^{(GSN118\text{-}120AAA\ SETGS157\text{-}161AAAAA)}$ mutant protein, which does not induce necrosis but retains PTI activity (Fig. 9). Collectively, our findings and work on additional cell death apoplastic NIPs show that induced cell death and plant defense-activation are not always linked.

A number of apoplastic effectors interact with plant RLPs and deliver the signals via a RLP-SOBIR1-BAK1 complex (Albert et al., 2015; Du et al., 2015; Liebrand et al., 2013; Ma et al., 2015; Postma et al., 2016; Zhang et al., 2014b; Zhang et al., 2013). Apoplastic effectors from the wheat pathogen *Z. tritici* were recently shown to induce NbBAK1 and NbSOBIR1-dependent cell death or chlorosis in non-host *N. benthamiana* plants (Kettles et al., 2017), indicating the centrality of RLPs-SOBIR1-BAK1 complexes in recognition and delivering of the signals of apoplastic effectors. While BcXYG1 is not a classical effector (it does not target the immune system), we nevertheless showed it is also targeted to the plant cell membrane, and its cell death effect is mediated by SOBIR1-BAK1. Hence, it is also logical to predict that BcXYG1 recognizes a yet unknown plant plasma membrane RLP, which mediates the signal. The *P. sojae* PsXEG1 (homolog of BcXYG1) affects pathogenicity of this Oomycete, and in this case the enzymatic activity is required (Ma et al., 2015). A glucanase inhibiting protein (GmGIP1) is produced by the plant, and specifically blocks PsXEG1 as a means of defense (Ma et al., 2017b). PsXLP1, a class 2 GH12 and a homolog of PsXEG1 that lacks necrosis-inducing activity, also binds the plant GmGIP1, thereby counteracting the plant protection. It is thus possible to speculate that BcXYG2, which is also expressed at early infection stages but does not induce necrosis, might act as a BcXYG1 decoy that neutralizes putative BcXYG1-inhibiting plant proteins.

Multiple sequence alignment of BcXYG1 and additional GH12 proteins revealed higher similarity of BcXYG1 to necrosis-inducing GH12 proteins than to BcXYG2 (Supplemental Fig.

S3A). Based on this analysis we classified GH12 proteins into two groups, those that are more closely related to BcXYG1 and those that are less conserved. Homology search of BcXYG1 in fungal genomes revealed the presence GH12 proteins of the first group in the genomes of all of the necrotrophic and hemibiotrophic plant pathogenic fungi that were included in this search, namely *Colletotrichum gloeosporioides*, *Magnaporthe oryzae*, *Cochliobolus heterostrophus*, and *S. sclerotiorum* (Supplemental Fig. S2). However, we did not find class 1 GH12 proteins in the biotrophic pathogens that we examined, including *B. graminis* f. sp. *hordei*, *U. maydis* and *Puccinia* spp., as well as in the human pathogen *C. albicans.* This finding suggests that BcXYG1 belongs to a specific subgroup of GH12 proteins, which may have evolved to facilitate disease of fungal pathogens by inducing necrosis. Because early necrosis has a negative effect on development of biotrophic pathogens, this class of proteins might have been removed from their genomes during evolution. In addition to mentioned pathogens, we also found homologs of BcXYG1 in saprotrophic fungi that colonize and grow on dead plant residues. While these species probably don't need the necrosis-inducing activity during their life cycle, they may benefit from the xyloglucan-degrading endoglucanase activity of these proteins.

The specific induction of the *bcxyg1* gene *in planta* and accumulation of high levels of the BcXYG1 protein during the early stage of infection connect BcXYG1 with *in planta* development and pathogenicity. Furthermore, we found homologues of BcXYG1 in necrotrophic and hemibiotrophic pathogens, which benefit from host cell death, but no in biotrophic pathogens, in which host cell death blocks infection. Despite these evidences, which support a role of BcXYG1 in *B. cinerea* pathogenicity, we did not observe differences in lesion size produced by *B. cinerea* deletion mutants that lack BcXYG1 (Supplemental Fig. S7). This result is not surprising in light of the presence of additional NIPs in the fungal secretome. Indeed, similar results were reported in analysis of other *B. cinerea* NIPs, such as BcNEP1/2 (Cuesta Arenas et al., 2010) and BcIEB1 (Frías et al., 2016).

Our working model predicts that NIPs are necessary for production of local necrosis during the early stage of infection. Accordingly, mutants in NIP-encoding genes are expected to be specifically affected in production of early necrosis, but not at the stage of spreading lesion. To determine possible effect of BcXYG1 in early stage of the disease, we analyzed infection of bean leaves using PathTrack©, a non-invasive, automated system for live imaging and quantitative measurement of disease development (Eizner et al., 2017). This analysis revealed that the leaves infected with the *BcXYG1* over expression strains OEXYG1 or OEMXYG1, produced earlier and more intense local necrosis. Importantly, later lesion expansion rate was unchanged compared with the wild type strain, which explains the similar lesion size at 72 hpi. This result shows the specific role of BcXYG1 in

generation of the early necrotic zone, which is necessary for initial disease establishment. Similarly, a NEP1 over expression strain also showed earlier and more intense necrosis (Fig. 5), supporting the general role of NIPs in disease establishment. Previous analysis of *nep1* deletion strains revealed no change in pathogenicity of the mutants, precluded determination of a role of this NIP in pathogenicity (Cuesta Arenas et al., 2010). Therefore, gain of function coupled with more detailed analysis of pathogenicity, e.g., using PathTrack© can reveal hidden roles of previously unrecognized pathogenicity factors such as NIPs and other types of effectors.

Several studies have reported that necrotrophic fungi, such as *B. cinerea*, *S. sclerotiorum* and *Plectosphaerella cucumerina*, might have a hemi-biotrophic phase that precedes killing of the host cells (Kabbage et al., 2013; Kabbage et al., 2015; Pétriacq et al., 2016; van Kan et al., 2014; Williamson et al., 2011). Indeed, necrotrophic pathogen, such as *P. cucumerina*, can shorten the biotrophic stage dependently of the spore densities at localized leaf areas during early infection, thereby gaining an advantage of immunity-related cell death in host plant (Pétriacq et al., 2016). According to this new definition, the signal exchange and type of interactions during this short phase may determine the outcome of infection. We did not observe a hemibiotrophic-like development in our experimental conditions, however there is a very short time period that lasts about 24 h in which hyphae develop on the surface of the plant without development of visible necrotic symptoms. This period is shortened in leaves infected by the BcXYG1 and MBcXYG1 expressing strains due to earlier secretion of BcXYG1. Despite the earlier appearance of initial necrotic spots in the over expression strains-infected leaves, disease progression was almost unaffected. A possible explanation for this result might be activation of the plant defense by BcXYG1, which counteract the cell death promoting activity. Accordingly, over expression of *bcxyg1* not only stimulates the production of local necrosis but also cause earlier activation of the plant defense. In our interpretation, the short, symptomless phase, which has been referred to as "hemi-biotrophic" is not synonym to a biotrophic phase, but rather to a phase in which the fungus grows on the surface of the leaf, thus avoiding a direct contact with the plant hostile environment, while releasing factors such as BcXYG1 that cause necrosis underneath. These factors, at the same time are recognized by the plant immune system leading to defense activation. Hence, constitutive over expression of NIPs may destroy the delicate balance between the fungus and host, and may have negative effects on disease progression despite earlier and increased levels of necrosis. This scenario is supported by results reported in the CA-BcRAC strain (Minz et al., 2013). This mutant shows earlier and markedly enhanced necrosis, however, lesion size at 72 hpi is slightly smaller than in wild type-infected leaves. Our current proteomic analysis showed high accumulation of several NIPs in secretome of the CA-BcRAC strain, including NPP1 (14.37 fold increase over wild

type secretome) and BcSpl1 (1.64 fold increase). BcSpl1 contributes necrosis-inducing activity and to virulence of *B. cinerea*, but it can also induce systemic resistance of host plant to pathogens (Frías et al., 2011; Frías et al., 2013).

The activation of defense by BcXYG1 probably involves signaling through the salicylic acid (SA) or JA jasmonic/ethylene (JA/ET) signalling pathways. SA signaling pathway is well known in the immune response against biotrophic pathogens, whereas the JA/ET pathway has been associated with the defense against necrotrophs (Durrant and Dong, 2004; Glazebrook, 2005; Grant and Lamb, 2006). Previous study has demonstrated that *B. cinerea* manipulates the antagonistic effects between SA and JA immune pathways to enhanced tomato susceptibility by secreting a β-(1,3)(1,6)-D-glucan (EPS), which can activate the SA signal pathway, which also inhibits JA signaling through NPR-1 (EI Oirdi et al., 2011). However, many studies have also shown that cross-talk between SA and JA/ET signaling pathways, either antagonistic and/or synergistic, can optimize the defense response against different classes of pathogens (Ferrari et al., 2003; Guo and Stotz, 2007; Koornneef and Pieterse, 2008; Mur et al., 2006; Spoel et al., 2007). We showed here that infiltration of leaves with BcXYG1 induces genes of both SA and JA signal pathways, indicating that BcXYG1 triggers the host plant defense response through multi-signal pathways. Similar results have demonstrated that several effectors and phytotoxin from *B. cinerea* and other pathogens can trigger both SA- and JA- mediated defense in plants (Rossi et al., 2011; Xiang et al., 2017; Zhang et al., 2017; Zhang et al., 2015). However, which signal pathway is more significant and the exact relationships among these signal pathways remain largely unknown and require further investigation.

MATERIALS AND METHODS

Fungi, Bacteria, Plants, Growth Conditions, and Inoculation

B. cinerea B05.10 wild type strain and derived mutants were used in this study (for details see Supplemental Table S1). All strains were routinely grown on potato dextrose agar (PDA, Acumedia) and maintained at 22°C under continuous fluorescent light supplemented with near UV (black) light. Conidia were obtained from 7-days-old cultures. *Escherichia coli* strain DH5α and Rosetta-gami (DE3) were used to propagate plasmids and express target proteins, respectively. *Agrobacterium tumefaciems* strain GV3101 was used for Agrobacterium-mediated transient expression of proteins in plant leaves. Bean (*Phaseolus vulgaris* cv. French bean, genotype N9059), tobacco (*Nicotiana benthamiana*), wheat (*Triticum aestivum*), and tomato (*Solanum lycopersicum*) plants were grown in a greenhouse [16 h : 8 h intervals of (25°C : 22°C, light : dark)].

Pathogenicity assays of *B. cinerea* on beans were performed as previously described

(Shlezinger et al., 2011). Conidia were collected from plates, washed and suspended in inoculation medium (Gamborg's B5 medium supplemented with 2% glucose and 10 mM KH_2PO_4/K_2HPO_4, pH 6.4). The primary leaves of 9-days-old beans were inoculated with 7.5 µl conidial suspensions (2×10^5 conidia/ml), the infected plants were incubated in a humid chamber at 22°C under fluorescent illumination for 72 h, and the lesions diameter was then measured. When specified, PathTrack© (Eizner et al., 2017) was used to determine infection kinetics and parameters.

Preparation of *B. cinerea* Secretome

Bean leaves were placed in glass trays with moist filter paper, and 50 ml of droplets of conidia suspension (5×10^5 conidia/ml) were applied on 50 leaves so that they covered the entire leaf. Inoculated leaves were incubated in a humid chamber at 22°C for 28 h and the inoculation suspension was then collected from the leaves, centrifuged at 4,000 *g* for 10 min at 4°C, and the supernatant was collected into a fresh tube. The samples were filtered through a 0.45 µm Minisart® non-pyrogenic filter (Sartorius-Stedim Biotech, Germany) to remove residual mycelia, conidia and plant residues, and then further purified using Amicon® Ultra-4 Centrifugal Filter Devices (4 ml, 10 kDa, Merck Millipore, Massachusetts, USA) to remove remnants of the inoculation medium and small toxins such as botrydial and other types of toxic molecules. The clean samples were dissolved in 4 ml Phosphate Buffer Saline (PBS) and stored at –80°C. To test for necrosis-inducing activity, the clean secretome was infiltrated into *N. benthamiana* leaves using a syringe, and necrosis development was determined after 48-96 h. For detection of proteins in secretome, samples were separated by Sodium Dodecyl Sulfate, Sodium Salt (SDS) gel electrophoresis and stained with silver reagent.

Proteomic Analysis

Sample Preparation

Purified secretome samples were frozen at -80°C and then lyophilized overnight using a Christ Delta 1-24 LSC Freeze Dryer lyophilizer (SciQuip, Newtown, Wem, Shropshire, United Kingdom). Dried proteins were resuspended in 8 M urea (Sigma, Saint Louis, Missouri, USA) with 0.1 M Tris-HCl, pH 7.9 on ice for 10 min. Proteins were reduced by incubation with dithiothreitol (5 mM; Sigma, Saint Louis, Missouri, USA) for 1 h at room temperature, and alkylated with 10 mM iodoacetamide (Sigma, Saint Louis, Missouri, USA) in the dark for 45 min. Samples were diluted to 2 M urea with 50mM ammonium bicarbonate. Proteins were then subjected to digestion with trypsin (Promega; Madison, WI, USA) overnight at 37°C (50:1 protein amount : trypsin), followed by a second trypsin digestion for 4 h. The digestions were stopped by addition of trifluroacetic acid (1%). Following digestion, peptides were desalted using solid-phase extraction columns (Oasis

612 HLB, Waters, Milford, MA, USA). The samples were stored at -80˚C until further analysis.

613 **Liquid Chromatography**

614 ULC/MS grade solvents were used for all chromatographic steps. Each sample was loaded
615 using split-less nano-Ultra Performance Liquid Chromatography (10 kpsi nanoAcquity; Waters,
616 Milford, MA, USA). The mobile phase was: A) H_2O + 0.1% formic acid and B) acetonitrile + 0.1%
617 formic acid. Desalting of the samples was performed online using a reversed-phase C18 trapping
618 column (180 µm internal diameter, 20 mm length, 5 µm particle size; Waters). The peptides were
619 then separated using a T3 HSS nano-column (75 µm internal diameter, 250 mm length, 1.8 µm
620 particle size; Waters) at 0.35 µl/min. Peptides were eluted from the column into the mass
621 spectrometer using the following gradient: 4% to 30% B in 105 min, 30% to 90% B in 5 min,
622 maintained at 90% for 5 min and then back to the initial conditions.

623 **Mass Spectrometry and Data Acquisition**

624 The nanoUPLC was coupled online through a nanoESI emitter (10 µm tip; New Objective;
625 Woburn, MA, USA) to a quadrupole orbitrap mass spectrometer (Q Exactive Plus, Thermo
626 Scientific) using a FlexIon nanospray apparatus (Proxeon). Data was acquired in DDA mode, using
627 a Top10 method. MS1 resolution was set to 70,000 (at 400 m/z) and maximum injection time was
628 set to 20 msec. MS2 resolution was set to 17,500 with maximum injection time of 60 msec.

629 **Data Processing and Analysis**

630 Raw data was imported into the Expressionist® software (Gene data) and processed as
631 previously described (Shalit et al., 2015). The software was used for retention time alignment and
632 peak detection of precursor peptides. A master peak list was generated from all MS/MS events and
633 sent for database search using Mascot v2.5 (Matrix Sciences). The data were searched against a
634 database containing protein sequences of *B. cinerea* downloaded from
635 http://www.broadinstitute.org/annotation/genome/botrytis_cinerea/MultiDownloads.html
636 (botrytis_cinerea__b05.10_vankan__1_proteins.fasta), as well as bean (*P. vulgaris*) and *A. thaliana*
637 protein sequences downloaded from Uniprot. Fixed modification was set to carbamidomethylation
638 of cysteines and variable modification was set to oxidation of methionine. Search results were then
639 filtered using the ProteinProphet algorithm (Nesvizhskii et al., 2003) to achieve maximum false
640 discovery rate of 1% at the protein level. Peptide identifications were imported back to
641 Expressionist to annotate identified peaks. Quantification of proteins from the peptide data was
642 performed using an in-house script (Shalit et al., 2015). Data was normalized based on the total ion
643 current. Protein abundance was calculated by summing the three most intense, unique peptides per
644 protein. A Student's *t*-Test, after logarithmic transformation, was used to identify significant

differences across the biological replica. Fold changes were calculated based on the ratio of arithmetic means of the case versus control samples.

Bioinformatics Analysis and Programs Used in This Study

The genomic sequence database of *B. cinerea* at JGI (http://genome.jgi.doe.gov/Botci1/Botci1.home.html) was used to characterize *B. cinerea* genes. The *SignalP 4.1 Server* (http://www.cbs.dtu.dk/services/SignalP/) and *SMART MODE* (http://smart.embl-heidelberg.de/smart/change_mode.pl) were used to analyze signal peptide sequence and protein domain. Databases *NCBI* and *UniProt* (http://www.uniprot.org/blast/) were used for Blastp analysis. The *Clustal W* and *Jalview* programs were used for mature proteins alignments. *MEGA 5* program was used to generate phylogenetic tree with unrooted neighbour-joining method. *PredictProtein* (https://www.predictprotein.org/) was used to predict disulfide bonds in protein. The *ASA-View* (http://www.abren.net/asaview/) was used to analyze the surface accessibility of protein. The 3D structural models were predicted using *I-TASSER* (http://zhanglab.ccmb.med.umich.edu/I-TASSER/).

Extraction and Manipulation of DNA and RNA

Relative gene expression levels were determined by quantitative RT-PCR (qRT-PCR) as previously described (Zhu et al., 2013). For measurement of *BcXYG1* gene expression during infection, bean leaves were sprayed with *B. cinerea* conidia (5×10^5 conidia/ml). Samples were obtained at 12, 24, 36, 48, 60 and 72 hpi, immediately frozen in liquid nitrogen, and stored at –80°C.

To compare *BcXYG1* transcript levels in different fungal strains, cultures were produced on PDA covered with cellophane, and the mycelia were collected after three days and stored at –80°C.

Genomic DNA of fungi was isolated using the NucleoSpin DNA kit (Macherey-Nagel, Germany) according to the manufacturer's instructions. Total plant and fungal RNA was isolated using the NucleoSpin RNA kit (Macherey-Nagel, Germany) according to the manufacturer's instructions and stored at –80°C. For cDNA synthesis, RNA samples were first treated with DNase I (Thermo Scientific, Lithuania), and the RevertAid™ First Strand cDNA Synthesis Kit (Thermo Scientific, Lithuania) was then used to generate the first strand cDNA.

qRT-PCR was performed using a CFX96 Touch™ Real-Time PCR Detection System (Bio-Rad, California, USA) and SYBR® Premix Ex Taq™ II (TAKARA Biotechnology, Dalian, China), according to the manufacturer's instructions. Primers were designed across or flanking an intron (Supplemental Table S2). The relative expression levels of the *B. cinerea Bcgpdh* gene (*BC1G_05277*) and the *P. vulgaris Actin-11* gene (GenBank: EH040443.1) were used as reference for normalizing the RNA sample. For each examined gene, qRT-PCR assays were repeated at least twice, each repetition with three independent replicates.

Plasmid Construction

Oligonucleotides used for plasmid construction are described in Supplemental Table S2. The *BcXYG1* replacement construct was generated as described (Ma et al., 2017a). The 5'(538 bp)- and 3'(534 bp)- flanks of the *BcXYG1* ORF were amplified by PCR from genomic DNA of the wild type strain B05.10 and the fragments were respectively cloned into the upstream and downstream of the *hph* cassette using Gibson Assembly Master Mix kit (New England Biolabs, Massachusetts, USA). To construct the *BcXYG1* over-expression vector, the full-length *BcXYG1* ORF fused with HA tag at the C terminus was cloned into the pH2G vector between the *B. cinerea* histone H2B promoter (*NCBI* ID: CP009806.1) and the endo-beta-1,4-glucanase precursor terminator (*NCBI* ID: CP009807.1).

To construct the *E. coli* protein expression vectors, the sequence encoding mature BcXYG1 protein without the signal peptide was cloned into pET-22b (+) (Novagen) to generate the expression vector pET22b-BcXYG1-6×His. For transient expression of proteins in plants using the Agrobacterium infiltration method, the sequence encoding *A. thaliana* PR3 (*TAIR* ID: AT3G12500) signal peptide was fused upstream of the BcXYG1-HA fusion protein, and the construct was cloned into pCAMBIA3300 (Cambia, Australia) between the CaMV 35S promoter and NOS terminator. Expressions vectors of additional genes were similarly constructed.

Characterization of *B. cinerea* Transformants

Transformation of *B. cinerea* was performed as previously described (Ma et al., 2017a). The following transgenic strains were produced: Δ*xyg1* (deletion of *BcXYG1*), OEXYG1 (over expression of an HA tagged native form of *BcXYG1*), OEMXYG1 (over expression of an HA tagged mutated form of *BcXYG1* that shows no enzymatic activity). Deletion of *BcXYG1* was confirmed by PCR using appropriate primers (Supplemental Table S2). Over expression of *BcXYG1* was determined by qRT-PCR and using the *Bcgpdh* (*BC1G_05277*) gene for normalizing the RNA sample. Two independent strains from *BcXYG1* deletion mutants (Δ*xyg1*-1 and Δ*xyg1*-2) were selected for growth and development characterization. To assay growth rates, strains were cultured on PDA at 22°C for 2 days, mycelial plugs were taken from the colony edge, placed in the center of a fresh PDA Petri dish, and incubated at 22°C either in light (24 h fluorescent light supplemented with near UV light) or in complete darkness. Colony morphology and sclerotia formation were monitored after 7 and 15 days, in light and dark-incubated cultures, respectively. For stress tolerance assay, examined strains were inoculated onto PDA plates containing 1 M NaCl, 1 M Sorbitol, 0.3 mg/ml Calcofluor White (CFW), 0.5 mg/ml Congo Red (CR) and 0.02% SDS, as previously described (Ma et al., 2017a).

Transient Expression, Protein Extractions and Immunoblot Analysis

Agrobacterium-mediated transient expression was performed using leaf infiltration, as previously described (Kettles et al., 2017). Proteins were extracted from *B. cinerea* and plants, and immunoblot analysis was performed as described (Wei et al., 2016). Briefly, approximately 0.2 g of tissue was ground to powder in liquid nitrogen and suspended in 1 ml lysis buffer (50 mM Tris pH 7.4, 150 mM NaCl, 1% Triton X–100, 1 mM EDTA, 1 mM PMSF). Samples were incubated on ice for 5 min and then centrifuged at 13,200 *g* for 10 min at 4°C to remove residues. The supernatant with the soluble proteins was mixed with 4×SDS sample buffer (40% Glycerol, 240 mM Tris-HCl pH 6.8, 8% SDS, 0.04% bromophenol blue, 5% beta-mercaptoethanol) and then denatured by boiling (100°C) for 5 min. Proteins were separated on SDS-PAGE, blotted onto membranes and the blots were analyzed using anti-HA or anti-His antibodies (Sigma, Saint Louis, Missouri, USA).

To confirm secretion of the BcXYG1-HA or MBcXYG1-HA fusion proteins by the transgenic strains, mycelia were cultured in PDB for three days, the medium was collected, filtered with 0.45 µm Minisart® non-pyrogenic filter (Sartorius-Stedim Biotech, Germany), and then frozen at –80°C and dried overnight using a lyophilizer. The dry powder was dissolved in 250 µl PBS and frozen at –80°C for further immunoblot analysis.

Expression, Purification and Enzyme Activity Analysis of Recombinant BcXYG1 Protein

E. coli strain Rosetta-gami (DE3) was used to express the recombinant proteins. Expression of the recombinant proteins in *E. coli* were performed according to Novagen pET System Manual 11th Edition. Purification of recombinant proteins was performed using Ni-NTA resin (GE Healthcare, Little Chalfont, Buckinghamshire, United Kingdom), as described (Zhang et al., 2015). Enzymatic activity of BcXYG1 and MBcXYG1 was determined at room temperature using xyloglucan (XG) as substrate in a final volume of 20 µl containing 50 mM ammonium acetate pH 5, 50 µg polysaccharide (XG from Tamarind, RG I, or RG II), and the examined protein. Following the enzymatic assays, the samples were dried by SpeedVac, resuspended in 200 µl ddH_2O and again dried using SpeedVac. Each dry sample was supplemented with 30 µl ddH_2O, vortexed, and kept at 8°C until MALDI analysis. For the MALDI analysis, 1 µl sample was spotted on the grid, while wet 1 µl of matrix was added and mixed. The matrix used was 1 µl DHB in MeOH. MALDI was carried out at the positive mode.

Protein Infiltration Assays and Induction of Plant Systemic Resistance by BcXYG1

To test the induction of plant necrosis by recombinant proteins produced in *E. coli*, BcXYG1 was dissolved in PBS and infiltrated into *N. benthamiana* leaves using a syringe. Plants were kept in a growth chamber at 25°C and photographed at 5 dpi. Additional treatments included infiltration with 100 µg/ml of MBcXYG1, EGFP and BcXYG2.

To test for induced systemic defense responses in plants, one of two primary leaves of 9-days-

old beans was infiltrated with 500 µl of 100 µg/ml examined protein. Treated plants were kept in a growth chamber for two days and the second (untreated) leaf was then inoculated with *B. cinerea* conidia, or was picked and stored at –80°C for RNA extraction and qRT-PCR analysis. Inoculated plants were incubated in a humid chamber at 22°C for additional 72 h and the lesions were then measured and photographed.

Protoplast Preparation and Assay

Tobacco protoplasts were prepared as previously described (Frías et al., 2014). To determine possible toxicity of MBcXYG1, protoplasts were incubated with 100 µg/ml protein at 25°C with gentle agitation at 60 rpm. The number of intact and damaged protoplasts was determined using a light microscope at 0, 2, 4, 6 and 8 h following addition of the protein.

Virus-Induced Gene Silencing (VIGS) in *N. benthamiana*

VIGS was used to test possible association of NbBAK1 and/or NbSOBIR1 with MBcXYG1-induced necrosis. *NbBAK1* or *NbSOBIR1* expression was silenced using VIGS, as previously described (Kettles et al., 2017). pTRV2-*GFP* was used as control and tobacco *NbBAK1* and *NbSOBIR1* expression levels were determined by qRT-PCR analysis as previously described (Franco-Orozco et al., 2017). Briefly, *A. tumefaciens* strain GV3101 harboring pTRV1, pTRV2-*GFP*, pTRV2-*NbBAK1* or pTRV2-*NbSOBIR1* constructs were cultured in LB medium containing 50 µg/ml Kanamycin and incubated at 28°C for 24 h. Bacteria cells were harvested by centrifugation at 5,000 *g,* washed twice in infiltration buffer (10 mM $MgCl_2$, 10 mM MES, pH 5.6), and cell density was adjusted to OD_{600} = 0.2. *A. tumefaciens* carrying either pTRV2-*NbBAK1* or pTRV2-*NbSOBIR1* plasmids was mixed at 1:1 ratio with a strain carrying the pTRV1 plasmid. Acetosyringone (Sigma, Saint Louis, Missouri, USA) was added to a final concentration of 200 µM, and the cultures were incubated at 28°C in the dark for 2 h and then infiltrated into *N. benthamiana* leaves using a 1 ml syringe. Virus-infected plants were maintained for 2-3 weeks in a growth chamber at 20°C and the uninoculated upper leaves of the plants were then treated with MBcXYG1 (+SP) using Agrobacterium-mediated transient expression method. The plants were moved to a growth chamber at 25°C and necrosis development was followed during the first five days after treatment.

Statistical Analysis

Statistical tests were performed using Origin 7.5 (OriginLab Corporation, Northampton, Massachusetts, USA). Data significance was analyzed by ANOVA (one-way, $P \leq 0.01$). In all graphs, results represent the mean value of 3–5 independent experiments ± SD (standard deviation). Different letters or asterisks in the graphs indicate statistical differences, $P \leq 0.01$.

781

782

ACKNOWLEDGMENTS

We thank Dr. Kostya Kanyuka in Rothamsted Research and Dr. Guido Sessa in Tel Aviv University for providing us the *A. tumefaciens* strains harboring the pTRV2-*NbBAK1*, pTRV2-*NbSOBIR1*, pTRV1 and pTRV2-*GFP* plasmids. The work was supported by BARD grants number CA9122-09 and IS4937-16 to Amir Sharon.

Figure Legends

Figure 1. Necrosis-inducing activity of *B. cinerea* secretome. A, Bean leaves were inoculated with suspension of *B. cinerea* spores. At the designated time points post inoculation, the suspension was collected and centrifuged, the spores and mycelia fragments were removed by filtering through 45 μm filters, and the clean suspension was infiltrated into *N. benthamiana* leaves. Images show leaves three days after treatment. B, Clean spore suspension was boiled, mixed with loading buffer, 20 μl were loaded on SDS-PAGE and separated by electrophoresis, and the gel was stained with silver reagent. C, Suspension was collected from inoculated bean leaves or from a fungus that was grown in Gamborg's B5 on a glass slide. Images were taken three days after infiltration of leaves with the clean suspensions. D, Clean suspension was treated by boiling for 10 minutes, precipitation of proteins with ammonium sulfate, or by dialysis through a 10 kDa membrane. Images were taken three days after infiltration of leaves with boiled suspension (boiled), suspension after protein precipitation [$(NH_4)_2SO_4$], dialyzed suspension (10 kDa), or the flow through after dialysis (flow through).

Figure 2. Purified BcXYG1 induces necrosis in multiple plants. *BcXYG1* and control proteins fused to 6×His were expressed in *E. coli,* purified, suspended in PBS and infiltrated into leaves. A, Immunoblot analysis of proteins expressed in *E. coli* using anti-His antibodies. EGFP-6×His: EGFP (negative control); BcXYG1-6×His: Native BcXYG1; MBcXYG1-6×His: mutant BcXYG1 that lacks enzymatic activity; BcXYG2-6×His: BcXYG1 homolog that lacks necrosis-inducing activity. B, Response of *N. benthamiana* leaves to different concentrations of BcXYG1-6×His. C, Treatment of *N. benthamiana* leaves with 100 μg/ml of purified proteins. D, Treatment of bean, tomato, wheat and maize leaves with 100 μg/ml of purified proteins. Images in B, C, and D were taken five days after treatment.

Figure 3. BcXYG1 is secreted to and is active in the plant apoplast. A, *B. cinerea* strains were cultured in liquid PDB medium for 48 h, the culture filtrate was collected and purified by filtration, and 20 μl were analyzed by gel electrophoresis and immunoblot using anti-HA antibodies.

OEXYG1: a *B. cinerea* transgenic strain over expressing HA-tagged native BcXYG1; OEMXYG1: a *B. cinerea* transgenic strain over expressing the enzymatic activity mutant protein MBcXYG1. Upper panel: immunoblot using anti-HA antibodies; bottom panel: Ponceau S staining of total proteins. (B-D) Analysis of necrosis produced by *A. tumefaciens* strains transiently expressing *BcXYG1* with and without secretion signal. B, Schematic presentation of the examined constructs. PR3 SP-BcXYG$^{19-248}$-HA: HA-tagged BcXYG1 with the native signal peptide replaced by *A. thaliana* PR3 secretion signal; ATG-BcXYG$^{19-248}$-HA: HA-tagged BcXYG1 lacking the native secretion signal; PR3 SP-BcXYG$^{23-398}$-HA: HA-tagged BcXYG2 (does not induce necrosis) with the native secretion signal replaced by *A. thaliana* PR3 secretion signal. C, Immunoblot analysis of proteins from *N. benthamiana* leaves transiently expressing the various constructs. PR3 SP-Nep1$^{21-246}$-HA: HA-tagged BcNep1-HA with the native secretion signal replaced by *A. thaliana* PR3 secretion signal; Control: *N. benthamiana* leaves infiltrated with GV3101 carrying a pCAMBIA3300 empty vector. Top panel: immunoblot using anti-HA antibodies; lower panel: Ponceau S staining of the Rubisco large subunit. D, Images of *N. benthamiana* leaves five days after infiltration with the various *A. tumefaciens*.

Figure 4. *BcXYG1* is highly expressed following plant inoculation. Bean leaves (black line) or Gamborg's B5 medium (red line) were inoculated with *B. cinerea* spores and expression levels of the *BcXYG1* and *BcXYG2* genes were evaluated by qRT-PCR. The *BcXYG1* and *BcXYG2* genes expression of *B. cinerea* inoculated on plants or in Gamborg's B5 medium plate at 0 h was set as level 1 and relative levels of transcript were calculated using the comparative Ct method. Transcript levels of the *B. cinerea Bcgpdh* gene were used to normalize different samples. Data represent means and standard deviations of three independent replications.

Figure 5. BcXYG1 contributes to establishment of the infection in early stages of pathogenic development. Bean leaves were inoculated with spores of the different strains, the leaves were photographed every 10 minutes and the data were analyzed using PathTrack© (Eizner et al., 2017). Images show selected time points during pathogenic development. Note earlier and more intense appearance of local lesions in over expression strains. Bar = 5mm in all of the images. The data show averages of time of first necrosis (1st necrosis), time when lesion spreading starts (break), and lesion expansion rate (Expn. Rate). Data represent the means and standard deviations from four independent experiments each with wild type and one of the mutants. Appearance of the first necrosis was significantly earlier ($p \leq 0.05$) in all of the over expression strains than in wild type, and was similar between the deletion and wild type strains, according to one way ANOVA. The

break time of the over expression strains was slightly earlier than break time of the wild type strain, however the differences were statistically insignificant ($p \leq 0.05$). Strain designation: wt- B05.10 wild type strain, Δ*bcxyg1* – deletion of the *bcxyg1* gene, OEXYG1 – over expression of the native *bcxyg1* gene, OEMXYG1 – over expression of the mutated (no enzymatic activity) *bcxyg1* gene, OENEP1 – over expression of the *bcnpp1* gene (NEP1).

Figure 6. BcXYG1 induces resistance in beans. A, One of the first two true leaves of a 9-day old bean seedling was infiltrated with 500 µl purified protein solution. The plants were kept in a growth chamber for 48h, the second leaf was then inoculated with wild type *B. cinerea* spores, and the plants were kept in humid environment. Pictures were taken (left) and average lesion size determined (right) 72 hpi. Data represent the means and standard deviations from three independent experiments, each with six replications. Different letters in the graph indicate statistical differences at $P \leq 0.01$ using ANOVA (one-way). B, Untreated leaves were picked 48 h after treatment and relative expression levels of the defense genes *Pvd1*, *PvPR1* and *PvPR2* were determined by qRT-PCR analysis. Expression in blank control plants was set as level 1. Expression level of *P. vulgaris Actin-11* gene was used to normalize different samples. Data represent means and standard deviations of three independent replicates.

Figure 7. Necrosis-inducing activity of BcXYG1 is dependent on the protein tertiary structure. A, Assessment of activity of denatured BcXYG1. Purified MBcXYG1 protein was incubated for 15 minutes at 25°C or 95°C. *N. benthamiana* leaves were treated with 100 µg/ml of the native (left) or denatured (right) proteins. Pictures were taken five days after the treatment of leaves. B, Assessment of the effect of destabilization of the tertiary structure on activity BcXYG1. *N. benthamiana* leaves were infiltrated with *A. tumefaciens* strains expressing constructs of MBcXYG1 with mutations that destroy the tertiary structure of the protein. Pictures were taken five days after treatment. MBcXYG1^{C33A}-HA: mutation in cysteine residue 33; MBcXYG1^{C61A}-HA: mutation in cysteine residue 61; MBcXYG1$^{C33A\ C61A}$-HA: mutation in both cysteine residues 33 and 61. C, Immunoblot analysis of proteins from *N. benthamiana* leaves transiently expressing cysteine residues mutants BcXYG1^{C33A}-HA, BcXYG1^{C61A}-HA and BcXYG1$^{C33A\ C61A}$-HA from a pCAMBIA3300 vector. HA-tagged proteins were detected using anti-HA antibodies, Ponceau S stained blots show the Rubisco large subunit. D, 3D structural models of BcXYG1 predicted using *I-TASSER* (http://zhanglab.ccmb.med.umich.edu/I-TASSER/) and further analyzed by *PyMOL* software. Left panel: a cartoon model of BcXYG1; right panel: the surface model of BcXYG1. The 12 C terminal amino acids constituting a β-strand structure (VFKTTAYSVSLN, 237-248 amino

acid) are depicted in blue. E, Effect of destabilization of BcxYG1 by deletion of the 12 C terminal amino acids. Pictures were taken five days after infiltration with an *A. tumefaciens* strain expressing either the mutant protein MBcXYG1$^{19\text{-}236(\Delta 237\text{-}248)}$-HA (left) or a native form of MBcXYG1 (right). F, Immunoblot analysis of proteins from *N. benthamiana* leaves transiently expressing either the 12 C terminal amino acids deletion mutant MBcXYG1$^{19\text{-}236(\Delta 237\text{-}248)}$-HA or MBcXYG1.

Figure 8. Induction of necrosis by BcXYG1 is mediated by two surface-exposed loop motifs. A, Effect of mutations in surface exposed loops on necrosis-inducing activity of BcXYG1. *N. benthamiana* leaves were infiltrated with *A. tumefaciens* strains expressing constructs with mutations in several different surface exposed loops. Pictures were taken five days after treatment. B, Immunoblot analysis. HA-tagged proteins were detected using anti-HA antibodies, Ponceau S stained blots show the Rubisco large subunit. C, A diagram of BcXYG2$^{\text{NTT134-136GSN GWADG177-181SETGS}}$-HA in which BcXYG2 amino acids NTT$^{134\text{-}136}$ and GWADG$^{177\text{-}181}$ are substituted by BcXYG1 amino acids GSN$^{118\text{-}120}$ and SETGS$^{157\text{-}161}$, respectively (BcXYG2$^{\text{GSN SETGS}}$). D, Activity assay of BcXYG2$^{\text{GSN SETGS}}$-HA. *N. benthamiana* leaves were infiltrated with *A. tumefaciens* carrying the BcXYG2$^{\text{GSN SETGS}}$-HA construct (left) or an empty vector (right). Pictures were taken five days after treatment. E, Immunoblot analysis. BcXYG2$^{\text{GSN SETGS}}$-HA was detected using anti-HA antibodies, Ponceau S stained blots show the Rubisco large subunit.

Figure 9. Necrosis-inducing activity of MBcXYG1 is not linked to plant defense-stimulating activity. A, One of first two true leaves of 9-days-old bean seedlings was infiltrated with 500 µl of the indicated proteins at 100 µg/ml. After two days, the other leaf was inoculated with *B. cinerea,* the plants were incubated in a humid chamber and lesions were photographed and measured 72 hpi. Controls: untreated first leaf; BcXYG2; pretreatment with BcXYG2; MBcXYG1: enzyme inactive BcXYG1 protein; Mutant$^{118\text{-}120\ 157\text{-}161}$: enzyme and necrosis-inactive BcXYG1 protein in which the external loops 118-120 and 157-161 were mutated (MBcXYG1$^{\text{GSN118-120AAA SETGS157-161AAAAA}}$). Data represent the means and standard deviations from three independent experiments, each with six replications. Different letters in the graph indicate statistical differences at $p \leq 0.01$ using ANOVA (one-way). B, Relative expression of defense genes. RNA was extracted from the untreated leaf 48 h after treatment of the first leaf and the levels of the defense genes *Pvd1*, *PvPR1* and *PvPR2* were determined by qRT-PCR. Expression in blank control plants was set as 1. Expression level of the *P. vulgaris Actin-11* gene was used to normalize different samples. Data represent means and standard deviations of three independent replicates.

Figure 10. BcXYG1 triggers cell death on the plant cell membrane. *N. benthamiana* protoplasts were incubated with 100 μg/ml protein. A, The number of intact protoplasts was counted at the indicated time points. Data represent the means and standard deviations from three independent biological repeats with a total of 15 visual field for each treatment. B, Images of tobacco protoplasts 1 h after beginning of incubation. Bars = 10 μm.

Figure 11. Necrosis-inducing activity of BcXYG1 is mediated by *NbBAK1* and *NbSOBIR1*. TRV-based VIGS vectors were used to initiate silencing of *NbBAK1* (TRV:*NbBAK1*) and *NbSOBIR1* (TRV:*NbSOBIR1*). TRV:*GFP* was used as a control virus treatment in these experiments. A, Three weeks after initiation of VIGS, *MBcXYG1* (+SP) was transiently expressed in the gene-silenced leaves using Agrobacterium infiltration. Leaves were photographed three and five days after treatment. B, Immunoblot analysis of proteins from indicated *N. benthamiana* leaves transiently expressing MBcXYG1-HA. Upper panel: MBcXYG1-HA was detected using anti-HA antibodies; lower panel: Ponceau S stained blots showing the Rubisco large subunit. C, Tobacco *NbBAK1* and *NbSOBIR1* expression levels after VIGS treatment determined by qRT-PCR analysis. Expression level in control plants (TRV:*GFP*) was set as 1. *NbEF1α* was used as an endogenous control. Means and standard deviations from three biological replicates are shown. Asterisks indicate significant differences ($P \leq 0.01$).

Supplemental Data

Supplemental Figure 1. Distribution of proteins found in the *B. cinerea* secretome. Proteins

Supplemental Figure 2. Sequence similarities between BcXYG1 and other GH12 proteins.

Supplemental Figure 3. Multiple sequence alignment of BcXYG2 (BC1G_01008), which does not induce necrosis, BcXYG1, and other necrosis-inducing GH12 proteins.

Supplemental Figure 4. Enzymatic activity assay of BcXYG1 and MBcXYG1.

Supplemental Figure 5. The *BcXYG1* gene deletion strategy and confirmation in *B. cinerea*.

Supplemental Figure 6. *bcxyg1* transgenic strains do not show developmental defects and deletion of *bcexyg1* does not affect induction of necrosis by the *B. cinerea* secretome.

Supplemental Figure 7. Virulence analysis of *B. cinerea* transgenic strains.

Supplemental Figure 8. Surface accessibility analysis of BcXYG1.

Supplemental Figure 9. Treatment with Dukatalon causes cell death but does not induce plant systemic resistance.

952 **Supplemental Figure 10. Plant defense-stimulating activity of MBcXYG1 is dependent on its**
953 **tertiary structure**.
954
955

Supplemental Table 1. List of *B. cinerea* strains used in this study.

Supplemental Table 2. List of Oligonucleotides used in this study.

Supplemental Table 3. List of secreted proteins identified in the secretome of *B. cinerea* wild type strain. The necrosis-inducing proteins reported in previous studies were labeled with blue color and BcXYG1 was labeled with yellow color.

Supplemental Table 4. Comparison of proteins presence and abundance between mutant Δ*bcnoxA* and wild type strain.

Supplemental Table 5. Comparison of proteins presence and abundance between CA-BcRAC and wild type strain.

Supplemental Table 6. List of priority categories candidates that have been screened using Agrobacterium infiltration assay of *N. benthamiana* leaves.

LITERATURE CITED

1. Albert I, Böhm H, Albert M, Feiler CE, Imkampe J, Wallmeroth N, Brancato C, Raaymakers TM, Oome S, Zhang H *et al*. (2015) An RLP23-SOBIR1-BAK1complex mediates NLP-triggered immunity. Nat Plants 1: 15140
2. Benedetti M, Pontiggia D, Raggi S, Cheng Z, Scaloni F, Ferrari S, Ausubel FM, Cervone F, De Lorenzo G (2015) Plant immunity triggered by engineered in vivo release of oligogalacturonides, damage-associated molecular patterns. Proc Natl Acad Sci USA 112: 5533–5538
3. Blanco-Ulate B, Morales-Cruz A, Amrine KCH, Labavitch JM, Powell ALT, Cantu D (2014) Genome-wide transcriptional profiling of *Botrytis cinerea* genes targeting plant cell walls during infections of different hosts. Front Plant Sci 5: 435.
4. Böhm H, Albert I, Oome S, Raaymakers TM, Van den Ackerveken G, Nürnberger T (2014) A conserved peptide pattern from a widespread microbial virulence factor triggers pattern-induced immunity in *Arabidopsis*. PLoS Pathog 10: e1004491
5. Brito N, Espino JJ, González C (2006) The endo-beta-1,4-xylanase xyn11A is required for virulence in *Botrytis cinerea*. Mol Plant Microbe Interact 19: 25–32
6. Cantarel BL, Coutinho PM, Rancurel C, Bernard T, Lombard V, Henrissat B (2009) The carbohydrate-active enzymes database (CAZy): an expert resource for glycogenomics. Nucleic Acids Res 37: D233–D238
7. Cheng Y, Wu K, Yao J, Li S, Wang X, Huang L, Kang Z (2016) PSTha5a23, a candidate effector from the obligate biotrophic pathogen *Puccinia striiformis* f. *sp*. *tritici*, is involved in

plant defense suppression and rust pathogenicity. Environ Microbiol doi: 10.1111/1462-2920.13610. (Epub ahead of print).

8. Cuesta Arenas Y, Kalkman ERIC, Schouten A, Dieho M, Vredenbregt P, Uwumukiza B, Osés Ruiz M, van Kan JAL (2010) Functional analysis and mode of action of phytotoxic Nep1-like proteins of *Botrytis cinerea*. Physiol Mol Plant Pathol 74: 376–386
9. De Wit PJ (2016) Apoplastic fungal effectors in historic perspective; a personal view. New Phytol 212: 805–813
10. Du J, Verzaux E, Chaparro-Garcia A, Bijsterbosch G, Keizer LC, Zhou J *et al.* (2015) Elicitin recognition confers enhanced resistance to *Phytophthora infestans* in potato. Nat Plants 1: 15034
11. Du Y, Stegmann M, Misas Villamil JC (2016) The apoplast as battleground for plant-microbe interactions. New Phytol 209: 34–38
12. Durrant WE, Dong X (2004) Systemic acquired resistance. Annu Rev Phytopathol 42: 185–209
13. Eizner E, Ronen M, Gur Y, Gavish A, Zhu W, Sharon A (2017) Characterization of *Botrytis*-plant interactions using PathTrack© - an automated system for dynamic analysis of disease development. Mol Plant Pathol 18: 503–512
14. EI Oirdi M, EI Rahman TA, Rigano L, EI Hadrami A, Rodriguez MC, Daayf F, Vojnov A, Bouarab K (2011) *Botrytis cinerea* manipulates the antagonistic effects between immune pathways to promote disease development in tomato. The Plant Cell 23: 2405–2421
15. Espino JJ, Gutiérrez-Sánchez G, Brito N, Shah P, Orlando R, González C (2010) The *Botrytis cinerea* early secretome. Proteomics 10: 3020–3034
16. Fang A, Han Y, Zhang N, Zhang M, Liu L, Li S, Lu F, Sun W (2016) Identification and characterization of plant cell death-inducing secreted proteins from *Ustilaginoidea virens*. Mol Plant Microbe Interact 29: 405–416
17. Ferrari S, Plotnikova JM, Loren GD, Ausubel FM (2003) Arabidopsis local resistance to *Botrytis cinerea* involves salicylic acid and camalexin and requires EDS4 and PAD2, but not SID2, EDS5 or PAD4. The Plant J 35: 193–205
18. Ferrari S, Savatin DV, Sicilia F, Gramegna G, Cervone F, De Lorenzo G (2013) Oligogalacturonides: plant damage-associated molecular patterns and regulators of growth and development. Front Plant Sci 4: 49
19. Frías M, González M, González C, Brito N (2016) BcIEB1, a *Botrytis cinerea* secreted protein, elicits a defense response in plants. Plant Sci 250: 115–124
20. Frías M, Brito N, González M, González C (2014) The phytotoxic activity of the cerato-platanin BcSpl1 resides in a two-peptide motif in the protein surface. Mol Plant Pathol 15: 342–351

21. Frías M, Brito N, González C (2013) The *Botrytis cinerea* cerato-platanin BcSpl1 is a potent inducer of systemic acquired resistance (SAR) in tobacco and generates a wave of salicylic acid expanding from the site of application. Mol Plant Pathol 14:191–196
22. Frías M, González C, Brito N (2011) BcSpl1, a cerato-platanin family protein, contributes to *Botrytis cinerea* virulence and elicits the hypersensitive response in the host. New Phytol 192: 483–495
23. Furman-Matarasso N, Cohen E, Du Q, Chejanovsky N, Hanania U, Avni A (1999) A point mutation in the ethylene-inducing xylanase elicitor inhibits the beta-1-4-endoxylanase activity but not the elicitation activity. Plant Physiol 121: 345–351
24. Franco-Orozco B, Berepiki A, Ruiz O, Gamble L, Griffe LL, Wang S, Birch PR, Kanyuka K, Avrova A (2017) A new proteinaceous pathogen-associated molecular pattern (PAMP) identified in Ascomycete fungi induces cell death in Solanaceae. New Phytol doi: 10.1111/nph.14542. [Epub ahead of print]
25. Gao Y, Faris JD, Liu Z, Kim YM, Syme RA, Oliver RP, Xu SS, Friesen TL (2015) Identification and characterization of the SnTox6-*Snn6* interaction in the *Parastagonospora nodorum*-wheat pathosystem. Mol Plant Microbe Interact 28: 615–625
26. Glazebrook J (2005) Contrasting mechanisms of defense against biotrophic and necrotrophic pathogens. Annu Rev Phytopathol 43: 205–227
27. González C, Brito N, Sharon A (2016) *Botrytis*–the fungus, the pathogen and its management in agricultural systems. Springer International Publishing Switzerland 2016. Chapter 12: 229–246
28. Grant M, Lamb C (2006) Systemic immunity. Curr Opin Plant Biol 9: 414–420
29. Guo XM, Stotz HU (2007) Defense against *Sclerotinia sclerotiorum* in Arabidopsis is dependent on jasmonic acid, salicylic acid, and ethylene signaling. Mol Plant Microbe Interact 20: 1384–1395
30. Kabbage M, Williams B, Dickman MB (2013) Cell death control: The interplay of apoptosis and autophagy in the pathogenicity of *Sclerotinia sclerotiorum*. PLoS Pathog 9: e1003287
31. Kabbage M, Yarden O, Dickman MB (2015) Pathogenic attributes of *Sclerotinia sclerotiorum*: switching from a biotrophic to necrotrophic lifestyle. Plant Sci 233: 53–60
32. Kettles GJ, Bayon C, Canning G, Rudd JJ, Kanyuka K (2017) Apoplastic recognition of multiple candidate effectors from the wheat pathogen *Zymoseptoria tritici* in the nonhost plant *Nicotiana benthamiana.* New Phytol 213: 338–350
33. Koornneef A, Pieterse CMJ (2008) Cross talk in defense signaling. Plant Physiol 146: 839–844.
34. Kubicek CP, Starr TL, Glass NL (2014) Plant cell wall-degrading enzymes and their secretion in plant-pathogenic fungi. Annu Rev Phytopathol 52: 427–451

35. Liebrand TW, van den Berg GC, Zhang Z, Smit P, Cordewener JH, America AH, Sklenar J, Jones AM, Tameling WI, Robatzek S, Thomma BP, Joosten MH (2013) Receptor-like kinase SOBIR1/EVR interacts with receptor-like proteins in plant immunity against fungal infection. Proc Natl Acad Sci USA 110: 10010–10015
36. Lorang J, Kidarsa T, Bradford CS, Gilbert B, Curtis M, Tzeng SC, Maier CS, Wolpert TJ (2012) Tricking the guard: exploiting plant defense for disease susceptibility. Science 338: 659–662
37. Lorang JM, Sweat TA, Wolpert TJ (2007) Plant disease susceptibility conferred by a "resistance" gene. Proc Natl Acad Sci USA 104: 14861–14866
38. Ma L, Salas O, Bowler K, Oren-Young L, Bar-Peled M, Sharon A (2017a) Genetic alteration of UDP-rhamnose metabolism in *Botrytis cinerea* leads to accumulation of UDP-KDG that adversely affects development and pathogenicity. Mol Plant Pathol 18: 263–275
39. Ma Z, Song T, Zhu L, Ye W, Wang Y, Shao Y, Dong S, Zhang Z, Dou D, Zheng X, Tyler BM, Wang Y (2015) A *Phytophthora sojae* glycoside hydrolase 12 protein is a major virulence factor during soybean infection and is recognized as a PAMP. Plant Cell 27: 2057–2072
40. Ma Z, Zhu L, Song T, Wang Y, Zhang Q, Xia Y, Qiu M, Lin Y, Li H, Kong L, Fang Y, Ye W, Wang Y, Dong S, Zheng X, Tyler BM, Wang Y (2017b) A paralogous decoy protects *Phytophthora sojae* apoplastic effector PsXEG1 from a host inhibitor. Science 355: 710–714
41. Marianayagam NJ, Sunde M, Matthews JM (2004) The power of two: protein dimerization in biology. Trends Biochem Sci 29: 618–625
42. Master ER, Zheng Y, Storms R, Tsang A, Powlowski J (2008) A xyloglucan-specific family 12 glycosyl hydrolase from *Aspergillus niger*: recombinant expression, purification and characterization. Biochem J 411: 161–170
43. Minz-Dub A, Kokkelink L, Tudzynski B, Tudzynski P, Sharon A (2013) Involvement of *Botrytis cinerea* small GTPases BcRAS1 and BcRAC in differentiation, virulence and the cell cycle. Eukaryot Cell 12: 1609–1618
44. Mur LAJ, Kenton P, Atzorn R, Miersch O, Wasternack C (2006) The outcomes of concentration-specific interactions between salicylate and jasmonate signaling include synergy, antagonism, and oxidative stress leading to cell death. Plant Physiol 140: 249–262
45. Nesvizhskii AI, Keller A, Kolker E, Aebersold R (2003) A statistical model for identifying proteins by tandem mass spectrometry. Anal Chem 75:4646–4658
46. Noda J, Brito N, González C (2010) The *Botrytis cinerea* xylanase Xyn11A contributes to virulence with its necrotizing activity, not with its catalytic activity. BMC Plant Biol 10: 38
47. Oliver RP, Friesen TL, Faris JD, Solomon PS (2012) *Stagonospora nodorum*: from pathology to genomics and host resistance. Annu Rev Phytopathol 50: 23–43

48. Oome S, Raaymakers TM, Cabral A, Samwel S, Böhm H, Albert I, Nürnberger T, Van den Ackerveken G (2014) Nep1-like proteins from three kingdoms of life act as a microbe-associated molecular pattern in *Arabidopsis*. Proc Natl Acad Sci USA 111: 16955–16960
49. Oliver RP, Solomon PS (2010) New developments in pathogenicity and virulence of necrotrophs. Curr Opin Plant Biol 13: 415–419
50. Ottmann C, Luberacki B, Küfner I, Koch W, Brunner F *et al.* (2009) A common toxin fold mediates microbial attack and plant defense. Proc Natl Acad Sci USA 106: 10359–10364
51. Pétriacq P, Stassen JH, Ton J (2016) Spore density determines infection strategy by the plant pathogenic fungus *Plectosphaerella cucumerina*. Plant Physiol 170: 2325–2339
52. Poinssot B, Vandelle E, Bentéjac M, Adrian M, Levis C, Brygoo Y, Garin J, Sicilia F, Coutos-Thévenot P, Pugin A (2003) The endopolygalacturonases 1 from *Botrytis cinerea* activates grapevine defense reactions unrelated to its enzymatic activity. Mol Plant Microbe Interact 16: 553–564
53. Postma J, Liebrand TWH, Bi G, Evrard A, Bye RR, Mbengue M, Kuhn H, Joosten MHAJ, Robatzek S (2016) Avr4 promotes Cf-4 receptor-like protein association with the BAK1/SERK3 receptor-like kinase to initiate receptor endocytosis and plant immunity. New Phytol 210: 627–642
54. Rossi FR, Gárriz A, Marina M, Romero FM, Gonzalez ME, Collado IG, Pieckenstain FL (2011) The sesquiterpene botrydial produced by *Botrytis cinerea* induces the hypersensitive response on plant tissues and its action is modulated by salicylic acid and jasmonic acid signaling. Mol Plant Microbe Interact 24: 888–896
55. Sandgren M, Shaw A, Ropp TH, Wu S, Bott R, Cameron AD, Ståhlberg J, Mitchinson C, Jones TA (2001) The X-ray crystal structure of the *Trichoderma reesei* family 12 endoglucanase 3, Cel12A, at 1.9 A resolution. J Mol Biol 308: 295–310
56. Sandgren M, Ståhlberg J, Mitchinson C (2005) Structural and biochemical studies of GH family 12 cellulases: improved thermal stability, and ligand complexes. Prog Biophys Mol Bio 89: 246–291
57. Segmüller N, Kokkelink L, Giesbert S, Odinius D, van Kan J, Tudzynski P (2008) NADPH oxidases are involved in differentiation and pathogenicity in *Botrytis cinerea*. Mol Plant Microbe Interact 21: 808–819
58. Sevier CS, Kaiser CA (2002) Formation and transfer of disulphide bonds in living cells. Nat Rev Mol Cell Bio 3: 836–847
59. Shalit T, Elinger D, Savidor A, Gabashvili A, Levin Y (2015) MS1-based label-free proteomics using a quadrupole orbitrap mass spectrometer. J Proteome Res 14: 1979–1986

60. Shi G, Friesen TL, Saini J, Xu SS, Rasmussen JB, Faris JD (2015) The wheat *Snn7* gene confers susceptibility on recognition of the *Parastagonospora nodorum* necrotrophic effector SnTox7. The Plant Genome 8: 1–10
61. Shlezinger N, Minz A, Gur Y, Hatam I, Dagdas YF *et al*. (2011) Anti-apoptotic machinery protects the necrotrophic fungus *Botrytis cinerea* from host-induced apoptotic-like cell death during plant infection. PLoS Pathog 7: e1002185
62. Spoel SH, Johnson JS, Dong X (2007) Regulation of tradeoffs between plant defenses against pathogens with different lifestyles. Proc Natl Acad Sci USA 104: 18842–18847
63. Trouvelot S, Héloir MC, Poinssot B, Gauthier A, Paris F, Guillier C *et al.* (2014) Carbohydrates in plant immunity and plant protection: roles and potential application as foliar sprays. Front Plant Sci 5: 592
64. van Kan JAL, Shaw MW, Grant-Downton RT (2014) *Botrytis* species: relentless necrotrophic thugs or endophytes gone rogue? Mol Plant Pathol 15: 957–961
65. Wei W, Zhu W, Cheng J, Xie J, Jiang D, Li G, Chen W, Fu Y (2016) Nox complex signal and MAPK cascade pathway are cross-linked and essential for pathogenicity and conidiation of mycoparasite *Coniothyrium minitans*. Sci Rep 6: 24325
66. Williams B, Kabbage M, Kim HJ, Britt R, Dickman MB (2011) Tipping the balance: *Sclerotinia sclerotiorum* secreted oxalic acid suppresses host defenses by manipulating the host redox environment. PLoS Pathog 7: e1002107
67. Williamson B, Tudzynski B, Tudzynski P, van Kan JA (2007) *Botrytis cinerea*: the cause of grey mould disease. Mol Plant Pathol 8: 561–580
68. Wu J, Wang Y, Park SY, Kim SG, Yoo JS, Park S, Gupta R, Kang KY, Kim ST (2016) Secreted alpha-N-arabinofuranosidase B protein is required for the full virulence of *Magnaporthe oryzae* and triggers host defences. PLoS ONE 11: e0165149
69. Xiang J, Li X, Yin L, Liu Y, Zhang Y, Qu J, Lu J (2017) A candidate RxLR effector from *Plasmopara viticola* can elicit immune responses in *Nicotiana benthamiana*. BMC Plant Biol 17: 75
70. Zhang H, Wu Q, Cao S, Zhao T, Chen L, Zhuang P, Zhou X, Gao Z (2014a) A novel protein elicitor (SsCut) from *Sclerotinia sclerotiorum* induces multiple defense responses in plants. Plant Mol Biol 86: 495–511
71. Zhang L, Kars I, Essenstam B, Liebrand TW, Wagemakers L, Elberse J *et al.* (2014b) Fungal endopolygalacturonases are recognized as microbe-associated molecular patterns by the *Arabidopsis* receptor-like protein RESPONSIVENESS TO BOTRYTIS POLYGALACTURONASES1. Plant Physiol 164: 352–364

72. Zhang L, Ni H, Du X, Wang S, Ma XW, Nürnberger T, Guo HS, Hua C (2017) The *Verticillium*-specific protein VdSCP7 localizes to the plant nucleus and modulates immunity to fungal infections. New Phytol doi: 10.1111/nph.14537. [Epub ahead of print]
73. Zhang W, Fraiture M, Kolb D, Loffelhardt B, Desaki Y, Boutrot FF *et al.* (2013) *Arabidopsis* receptor-like protein 30 and receptor-like kinase suppressor of BIR1-1/EVERSHED mediate innate immunity to necrotrophic fungi. Plant Cell 25: 4227–4241
74. Zhang Y, Zhang Y, Qiu D, Zeng H, Guo L, Yang X (2015) BcGs1, a glycoprotein from *Botrytis cinerea*, elicits defence response and improves disease resistance in host plants. Biochem Bioph Res Co 457: 627–634
75. Zhu W, Wei W, Fu Y, Cheng J, Xie J, Li G, Yi X, Kang Z, Dickman MB, Jiang D (2013) A secretory protein of necrotrophic fungus *Sclerotinia sclerotiorum* that suppresses host resistance. PLoS ONE 8: e53901

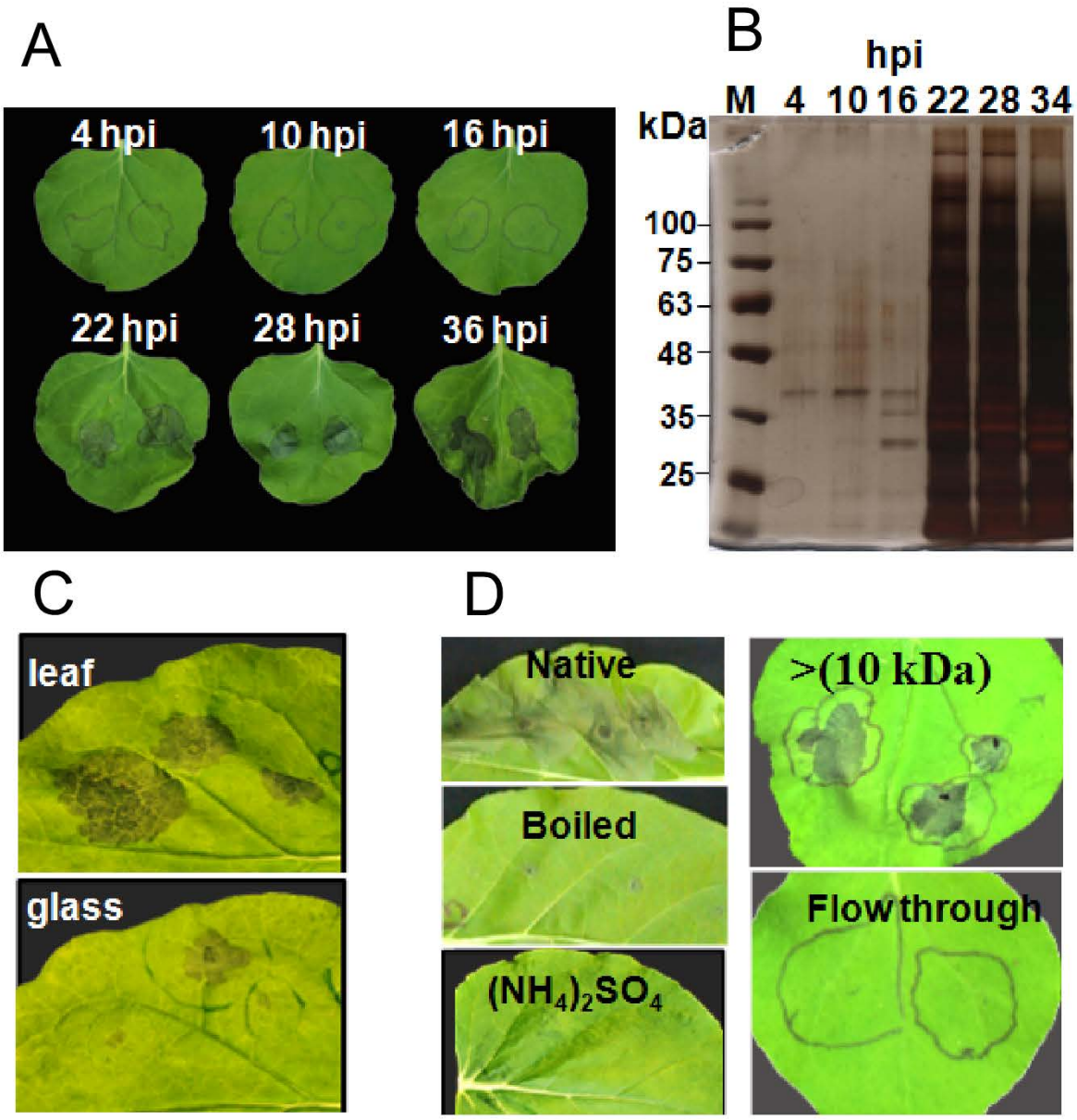

Figure 1. Necrosis-inducing activity of *B. cinerea* secretome. A, Bean leaves were inoculated with suspension of *B. cinerea* spores. At the designated time points post inoculation, the suspension was collected and centrifuged, the spores and mycelia fragments were removed by filtering through 45 µm filters, and the clean suspension was infiltrated into *N. benthamiana* leaves. Images show leaves three days after treatment. B, Clean spore suspension was boiled, mixed with loading buffer, 20 µl were loaded on SDS-PAGE and separated by electrophoresis, and the gel was stained with silver reagent. C, Suspension was collected from inoculated bean leaves or from a fungus that was grown in Gamborg's B5 on a glass slide. Images were taken three days after infiltration of leaves with the clean suspensions. D, Clean suspension was treated by boiling for 10 minutes, precipitation of proteins with ammonium sulfate, or by dialysis through a 10 kDa membrane. Images were taken three days after infiltration of leaves with boiled suspension (boiled), suspension after protein precipitation [$(NH_4)_2SO_4$], dialyzed suspension (10 kDa), or the flow through after dialysis (flow through).

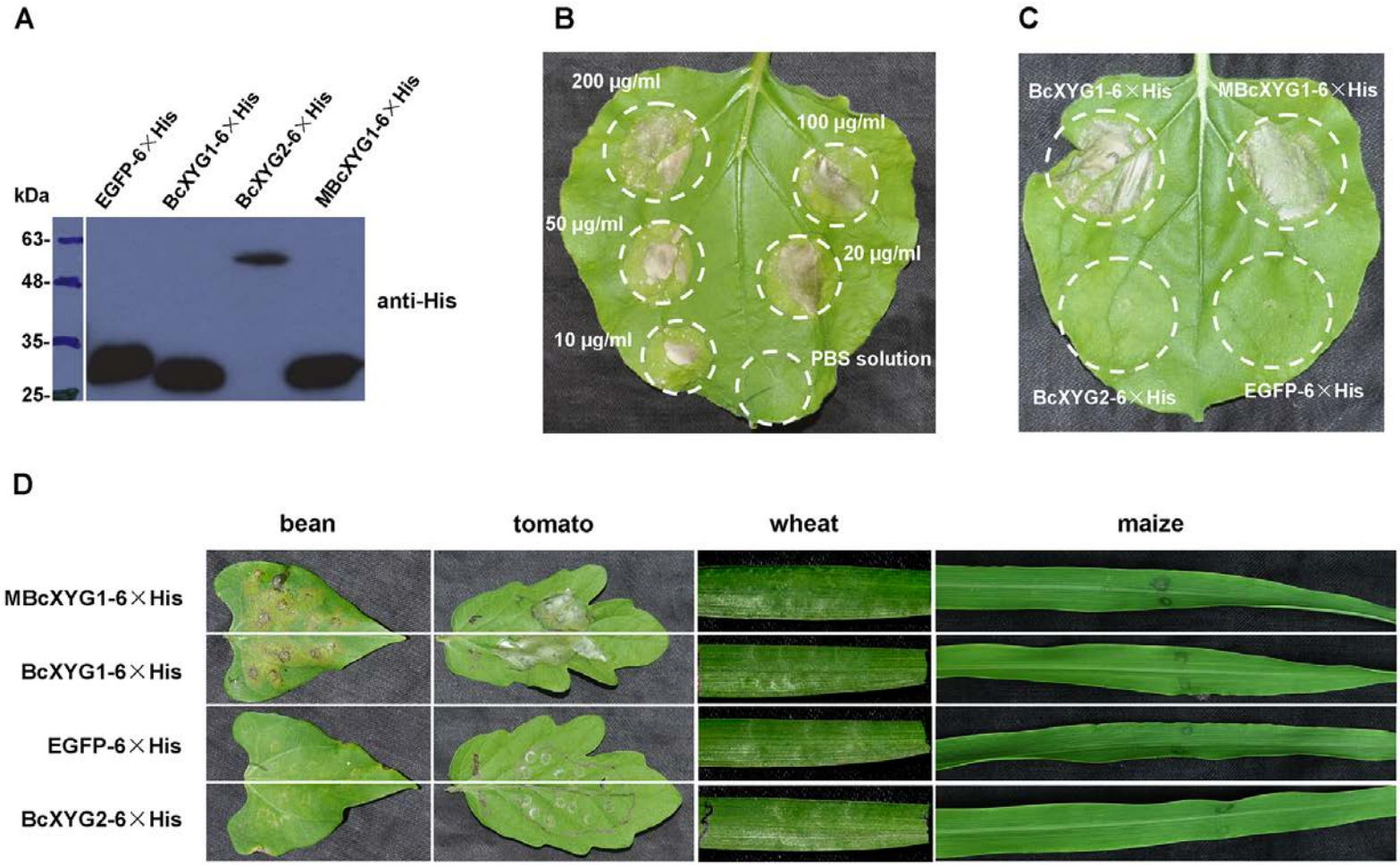

Figure 2 Purified BcXYG1 induces necrosis in multiple plants. *BcXYG1* and control proteins fused to 6xHis were expressed in *E. coli*, purified, suspended in PBS and infiltrated into leaves. A, Immunoblot analysis of proteins expressed in *E. coli* using anti-His antibodies. EGFP-6×His: EGFP (negative control); BcXYG1-6×His: Native BcXYG1; MBcXYG1-6×His: mutant BcXYG1 that lacks enzymatic activity; BcXYG2-6×His: BcXYG1 homolog that lacks necrosis-inducing activity. B, Response of *N. benthamiana* leaves to different concentrations of BcXYG1-6×His. C, Treatment of *N. benthamiana* leaves with 100 μg/ml of purified proteins. D, Treatment of bean, tomato, wheat and maize leaves with 100 μg/ml of purified proteins. Images in B, C, and D were taken five days after treatment.

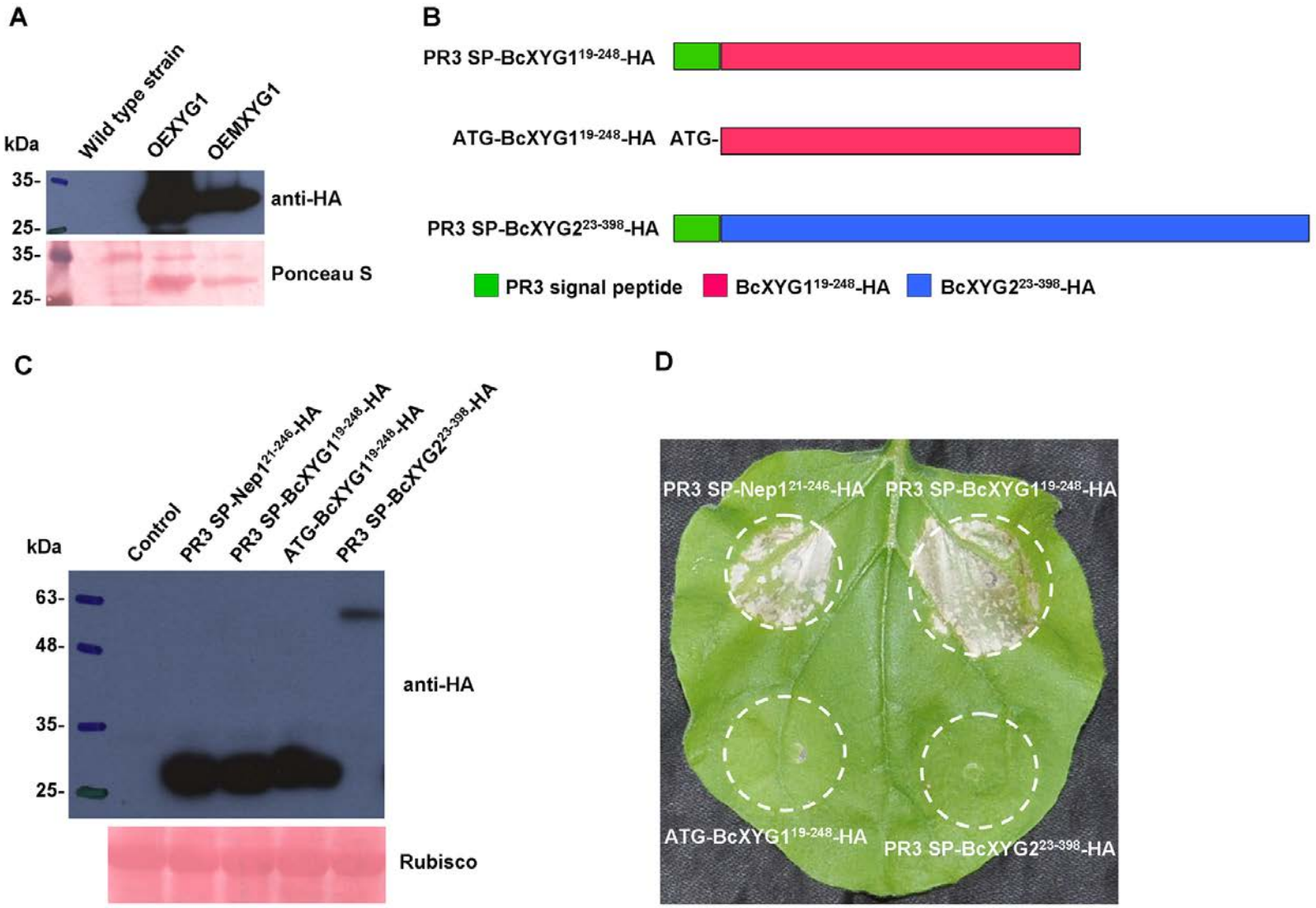

Figure 3 BcXYG1 is secreted to and is active in the plant apoplast. A, *B. cinerea* strains were cultured in liquid PDB medium for 48 h, the culture filtrate was collected and purified by filtration, and 20 µl were analyzed by gel electrophoresis and immunoblot using anti-HA antibodies. OEXYG1: a *B. cinerea* transgenic strain over expressing HA-tagged native BcXYG1; OEMXYG1: a *B. cinerea* transgenic strain over expressing the enzymatic activity mutant protein MBcXYG1. Upper panel: immunoblot using anti-HA antibodies; bottom panel: Ponceau S staining of total proteins. (b-d) Analysis of necrosis produced by *A. tumefaciens* strains transiently expressing *BcXYG1* with and without secretion signal. B, Schematic presentation of the examined constructs. PR3 SP-BcXYG$^{19\text{-}248}$-HA: HA-tagged BcXYG1 with the native signal peptide replaced by *A. thaliana* PR3 secretion signal; ATG-BcXYG$^{19\text{-}248}$-HA: HA-tagged BcXYG1 lacking the native secretion signal; PR3 SP-BcXYG$^{23\text{-}398}$-HA: HA-tagged BcXYG2 (does not induce necrosis) with the native secretion signal replaced by *A. thaliana* PR3 secretion signal. C, Immunoblot analysis of proteins from *N. benthamiana* leaves transiently expressing the various constructs. PR3 SP-Nep1$^{21\text{-}246}$-HA: HA-tagged BcNep1-HA with the native secretion signal replaced by *A. thaliana* PR3 secretion signal; Control: *N. benthamiana* leaves infiltrated with GV3101 carrying a pCAMBIA3300 empty vector. Top panel: immunoblot using anti-HA antibodies; lower panel: Ponceau S staining of the Rubisco large subunit. D, Images of *N. benthamiana* leaves five days after infiltration with the various *A. tumefaciens*.

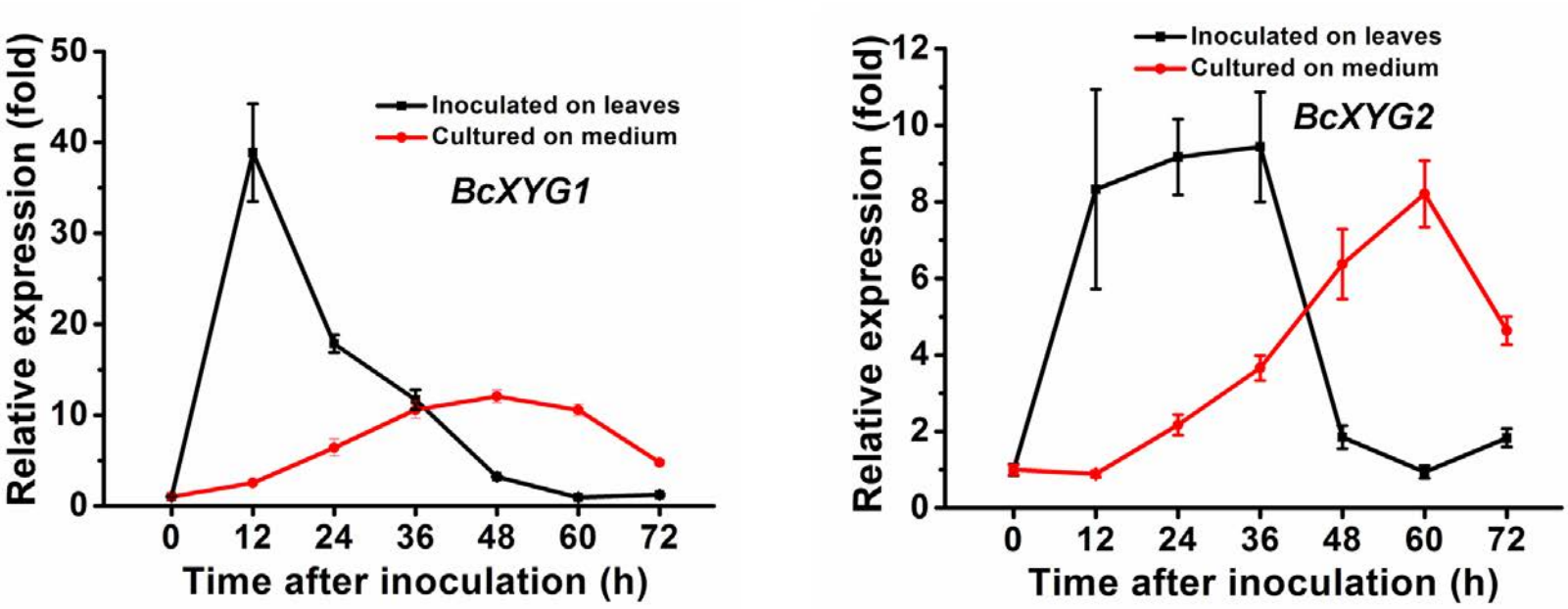

Figure 4 *BcXYG1* is highly expressed following plant inoculation. Bean leaves (black line) or Gamborg's B5 medium (red line) were inoculated with *B. cinerea* spores and expression levels of the *BcXYG1* and *BcXYG2* genes were evaluated by qRT-PCR. The *BcXYG1* and *BcXYG2* genes expression of *B. cinerea* inoculated on plants or in Gamborg's B5 medium plate at 0 h was set as level 1 and relative levels of transcript were calculated using the comparative Ct method. Transcript levels of the *B. cinerea Bcgpdh* gene were used to normalize different samples. Data represent means and standard deviations of three independent replications.

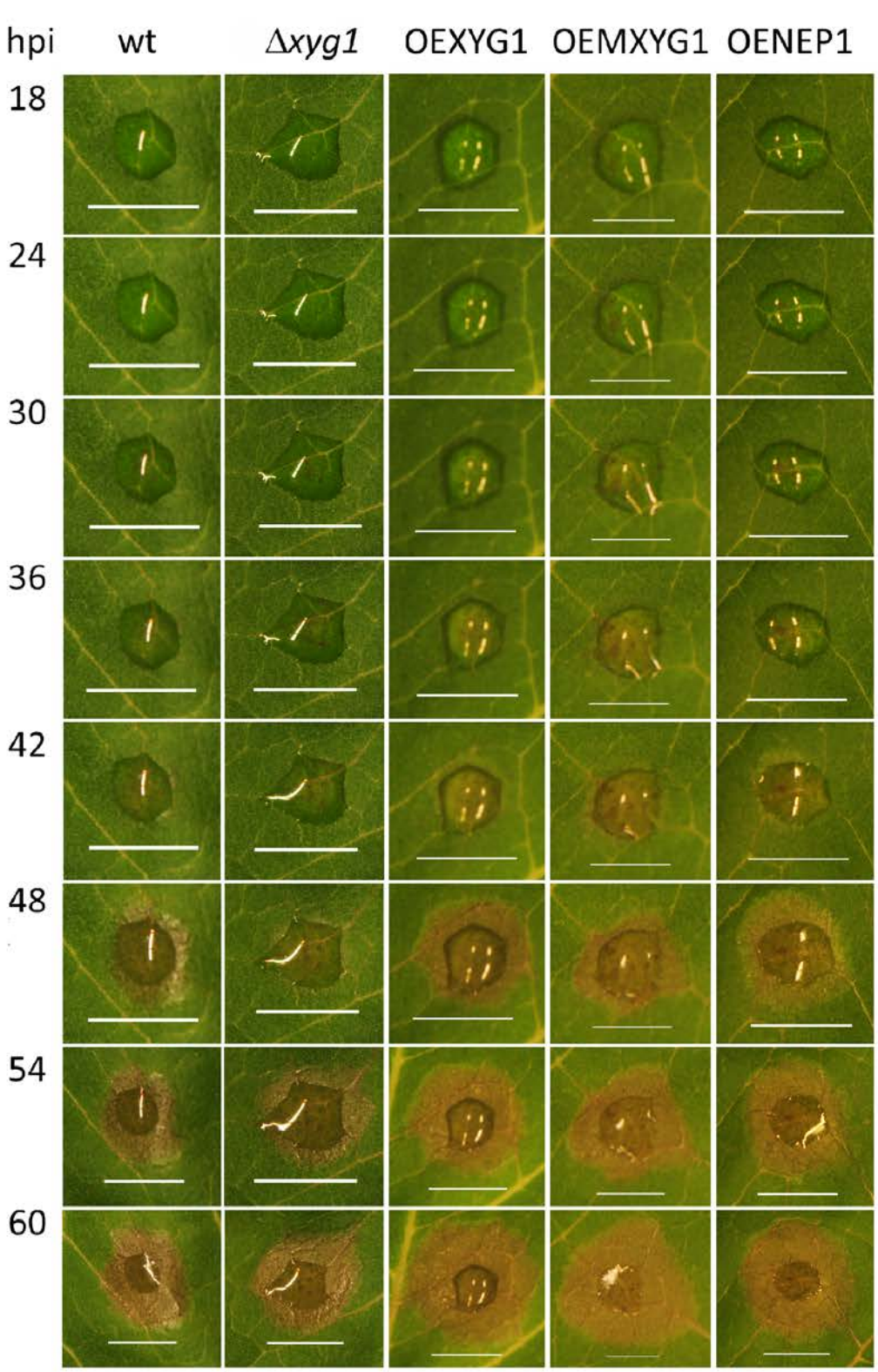

	wt	Δ*xyg1*	OEXYG1	OEMXYG1	OENEP1
1st necrosis (hpi)	26.50 ±1.91	26.70 ±1.50	17.25 ±2.22	18.50 ±2.52	20.50 ±2.89
Break (hpi)	43.62 ±2.62	44.12 ±2.46	39.25 ±0.96	40.50 ±3.41	39.50 ±1.73
Expn. Rate (mm/h)	0.159 ±0.018	0.167 ±0.008	0.158 ±0.027	0.167 ±0.008	0.177 ±0.020

Figure 5. BcXYG1 contributes to establishment of the infection in early stages of pathogenic development. Bean leaves were inoculated with spores of the different strains, the leaves were photographed every 10 minutes and the data were analyzed using PathTrack© (Eizner et al., 2017). Images show selected time points during pathogenic development. Note earlier and more intense appearance of local lesions in over expression strains. Bar = 5mm in all of the images. The data show averages of time of first necrosis (1st necrosis), time when lesion spreading starts (break), and lesion expansion rate (Expn. Rate). Data represent the means and standard deviations from four independent experiments each with wild type and one of the mutants. Appearance of the first necrosis was significantly earlier ($p = 0.05$) in all of the over expression strains than in wild type, and was similar between the deletion and wild type strains, according to one way ANOVA. The break time of the over expression strains was slightly earlier than break time of the wild type strain, however the differences were statistically insignificant ($p = 0.05$). Strain designations: wt – B05.10 wild type strain, Δ*xyg1* – deletion of the *bcxyg1* gene, OEXYG1 – over expression of the native *bcxyg1* gene, OEMXYG1 – over expression of the mutated (no enzymatic activity) *bcxyg1* gene, OENEP1 – over expression of the *bcnpp1* gene (NEP1).

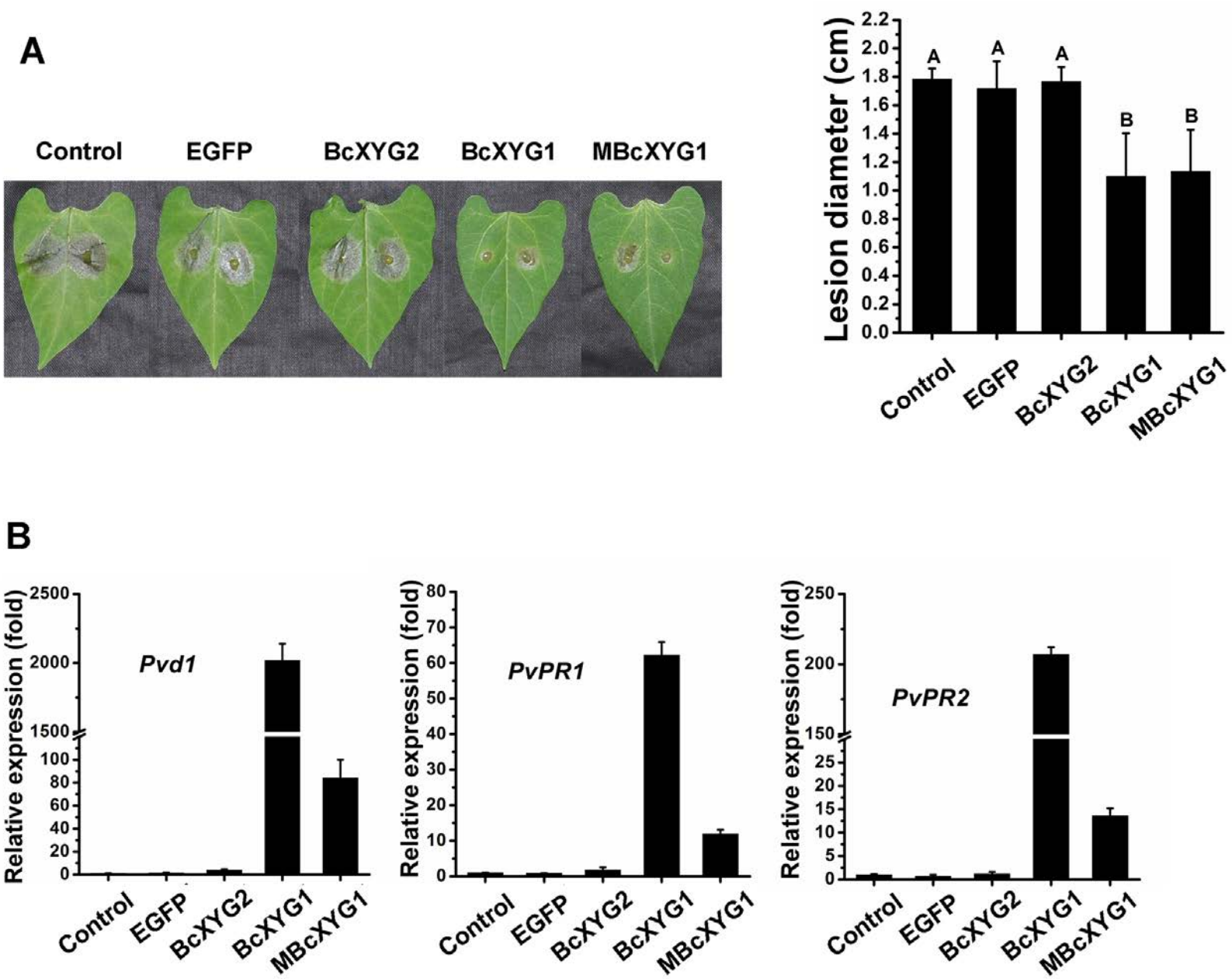

Figure 6 BcXYG1 induces resistance in beans. A, One of the first two true leaves of a 9-day old bean seedling was infiltrated with 500 µl purified protein solution. The plants were kept in a growth chamber for 48h, the second leaf was then inoculated with wild type *B. cinerea* spores, and the plants were kept in humid environment. Pictures were taken (left) and average lesion size determined (right) 72 hpi. Data represent the means and standard deviations from three independent biological repeats with a total of 18 leaves for each strain. Different letters in the graph indicate statistical differences at P = 0.01 using ANOVA (one-way). B, Untreated leaves were picked 48 h after treatment and relative expression levels of the defense genes *Pvd1*, *PvPR1* and *PvPR2* were determined by qRT-PCR analysis. Expression in blank control plants was set as level 1. Expression level of *P. vulgaris Actin-11* gene was used to normalize different samples. Data represent means and standard deviations of three independent replicates.

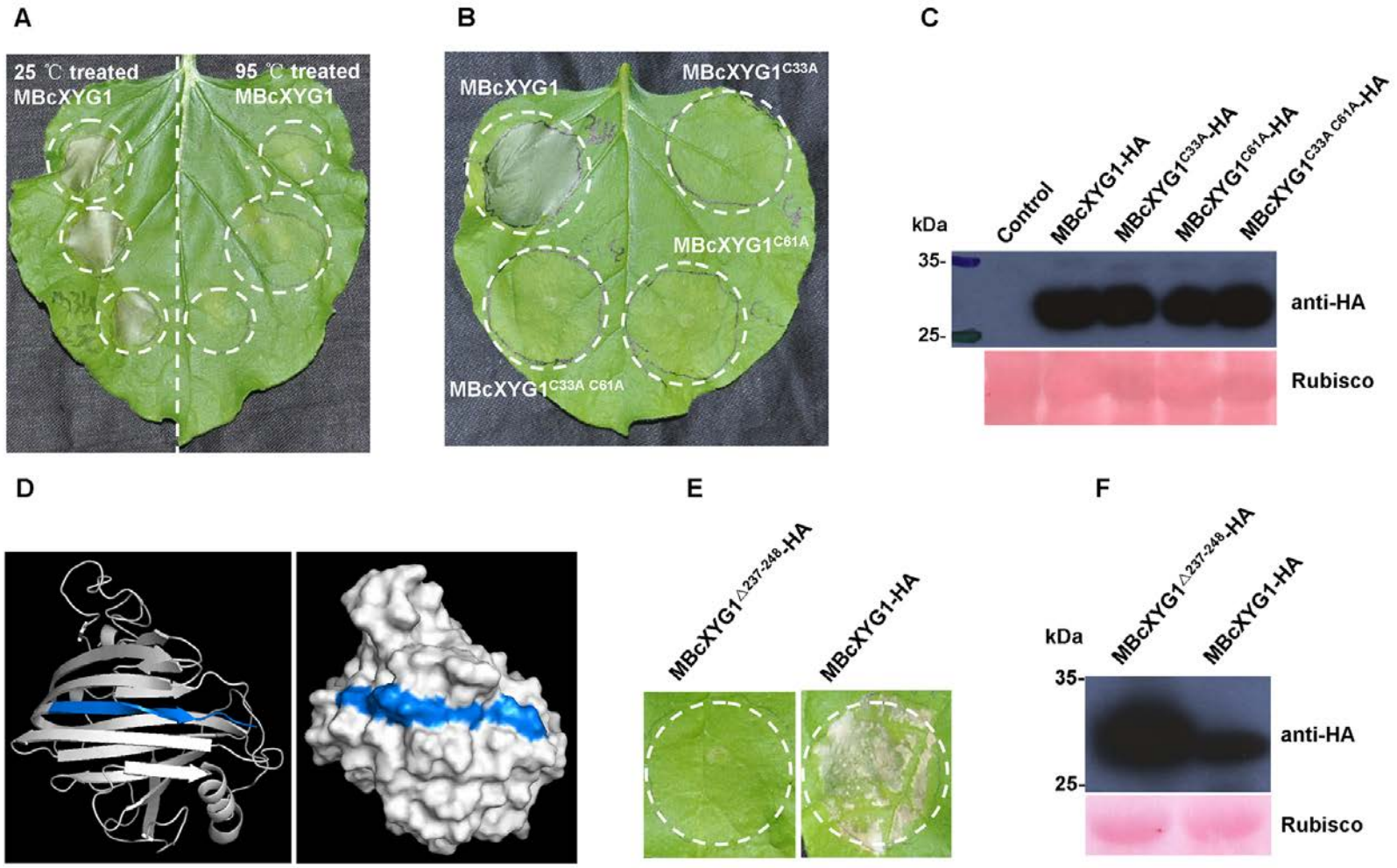

Figure 7 Necrosis-inducing activity of BcXYG1 is dependent on the protein tertiary structure. A, Assessment of activity of denatured BcXYG1. Purified MBcXYG1 protein was incubated for 15 minutes at 25°C or 95°C. *N. benthamiana* leaves were treated with 100 μg/ml of the native (left) or denatured (right) proteins. Pictures were taken five days after the treatment of leaves. B, Assessment of the effect of destabilization of the tertiary structure on activity BcXYG1. *N. benthamiana* leaves were infiltrated with *A. tumefaciens* strains expressing constructs of MBcXYG1 with mutations that destroy the tertiary structure of the protein. Pictures were taken five days after treatment. MBcXYG1^{C33A}-HA: mutation in cysteine residue 33; MBcXYG1^{C61A}-HA: mutation in cysteine residue 61; MBcXYG1$^{C33A\ C61A}$-HA: mutation in both cysteine residues 33 and 61. C, Immunoblot analysis of proteins from *N. benthamiana* leaves transiently expressing cysteine residues mutants BcXYG1^{C33A}-HA, BcXYG1^{C61A}-HA and BcXYG1$^{C33A\ C61A}$-HA from a pCAMBIA3300 vector. HA-tagged proteins were detected using anti-HA antibodies, Ponceau S stained blots show the Rubisco large subunit. D, 3D structural models of BcXYG1 predicted using *I-TASSER* (http://zhanglab.ccmb.med.umich.edu/I-TASSER/) and further analyzed by *PyMOL* software. Left panel: a cartoon model of BcXYG1; right panel: the surface model of BcXYG1. The 12 C terminal amino acids constituting a β-strand structure (VFKTTAYSVSLN, 237-248 amino acid) are depicted in blue. E, Effect of destabilization of BcxYG1 by deletion of the 12 C terminal amino acids. Pictures were taken five days after infiltration with an *A. tumefaciens* strain expressing either the mutant protein MBcXYG1$^{19\text{-}236(\Delta 237\text{-}248)}$-HA (left) or a native form of MBcXYG1 (right). F, Immunoblot analysis of proteins from *N. benthamiana* leaves transiently expressing either the 12 C terminal amino acids deletion mutant MBcXYG1$^{19\text{-}236(\Delta 237\text{-}248)}$-HA or MBcXYG1.

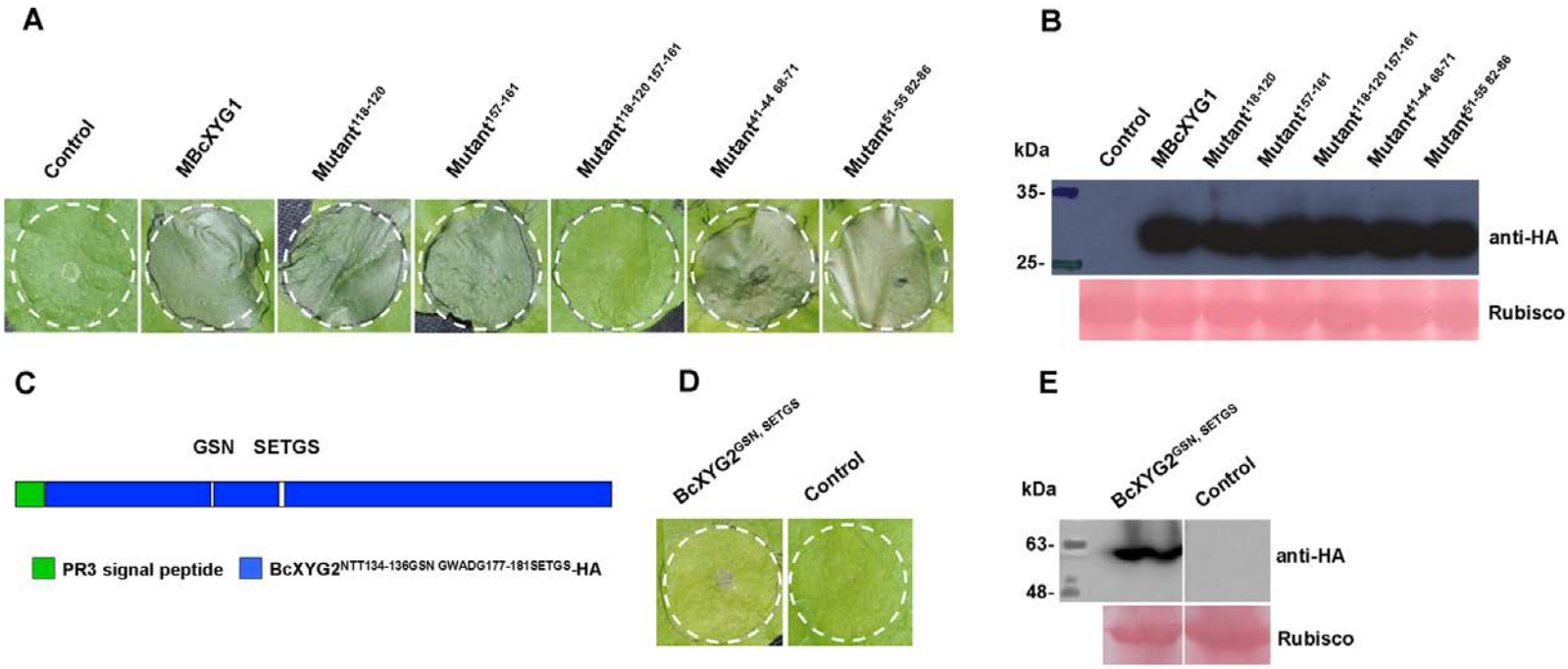

Figure 8 Induction of necrosis by BcXYG1 is mediated by two surface-exposed loop motifs. A, Effect of mutations in surface exposed loops on necrosis-inducing activity of BcXYG1. *N. benthamiana* leaves were infiltrated with *A. tumefaciens* strains expressing constructs with mutations in several different surface exposed loops. Pictures were taken five days after treatment. B, Immunoblot analysis. HA-tagged proteins were detected using anti-HA antibodies, Ponceau S stained blots show the Rubisco large subunit. C, A diagram of BcXYG2$^{NTT134-136GSN\ GWADG177-181SETGS}$-HA in which BcXYG2 amino acids NTT$^{134-136}$ and GWADG$^{177-181}$ are substituted by BcXYG1 amino acids GSN$^{118-120}$ and SETGS$^{157-161}$, respectively (BcXYG2$^{GSN\ SETGS}$). D, Activity assay of BcXYG2$^{GSN\ SETGS}$-HA. *N. benthamiana* leaves were infiltrated with *A. tumefaciens* carrying the BcXYG2$^{GSN\ SETGS}$-HA construct (left) or an empty vector (right). Pictures were taken five days after treatment. E, Immunoblot analysis. BcXYG2$^{GSN\ SETGS}$-HA was detected using anti-HA antibodies, Ponceau S stained blots show the Rubisco large subunit.

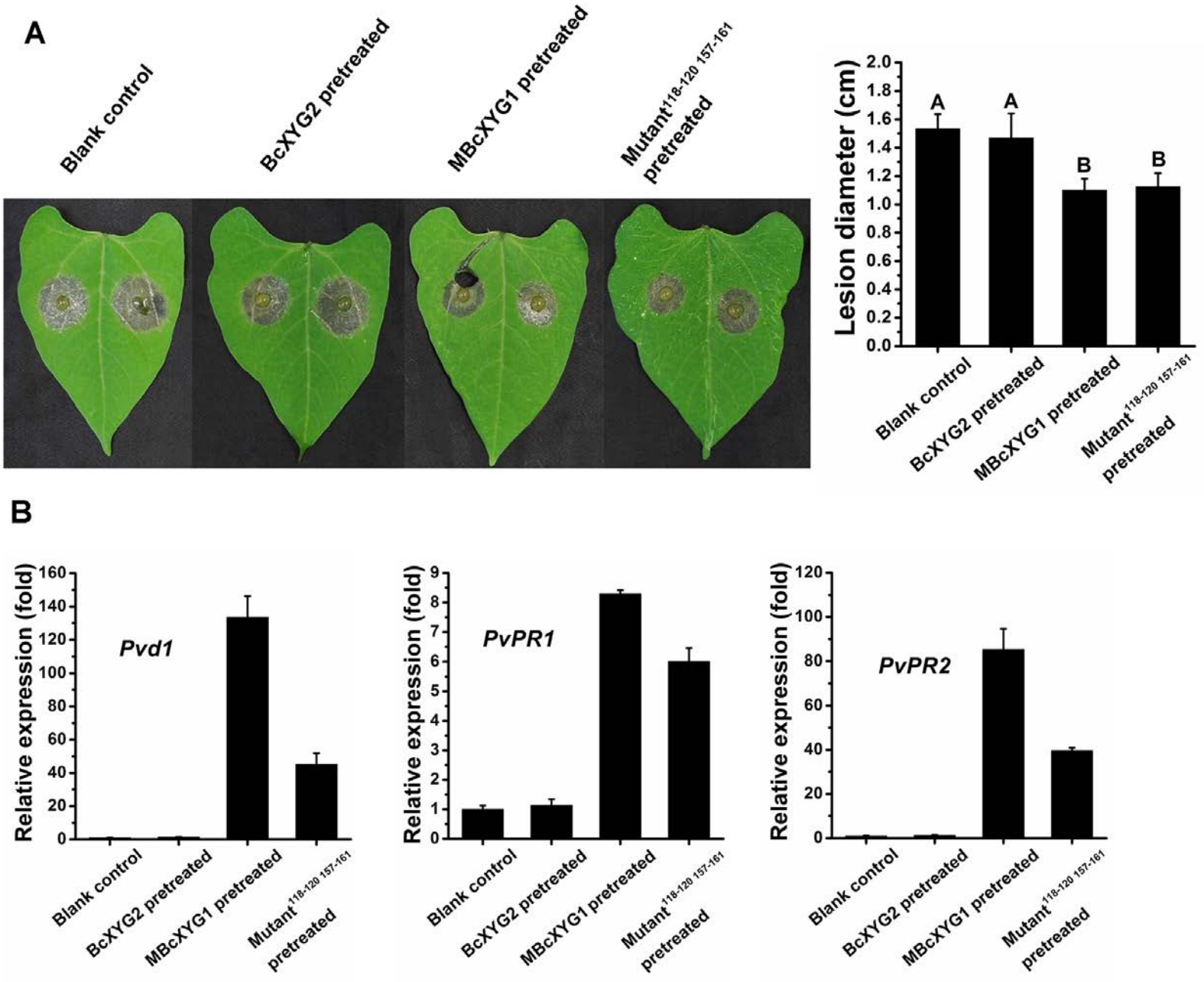

Figure 9 Necrosis-inducing activity of MBcXYG1 is not linked to plant defense-stimulating activity. A, One of first two true leaves of 9-days-old bean seedlings was infiltrated with 500 µl of the indicated proteins at 100 µg/ml. After two days, the other leaf was inoculated with *B. cinerea,* the plants were incubated in a humid chamber and lesions were photographed and measured 72 hpi. Controls: untreated first leaf; BcXYG2; pretreatment with BcXYG2; MBcXYG1: enzyme inactive BcXYG1 protein; Mutant$^{118\text{-}120\ 157\text{-}161}$: enzyme and necrosis-inactive BcXYG1 protein in which the external loops 118-120 and 157-161 were mutated (MBcXYG1$^{GSN118\text{-}120AAA\ SETGS157\text{-}161AAAAA}$). Data represent the means and standard deviations from three independent biological repeats with a total of 18 leaves for each strain. Different letters in the graph indicate statistical differences at P = 0.01 using ANOVA (one-way). B, Relative expression of defense genes. RNA was extracted from the untreated leaf 48 h after treatment of the first leaf and the levels of the defense genes *Pvd1*, *PvPR1* and *PvPR2* were determined by qRT-PCR. Expression in blank control plants was set as 1. Expression level of the *P. vulgaris Actin-11* gene was used to normalize different samples. Data represent means and standard deviations of three independent replicates.

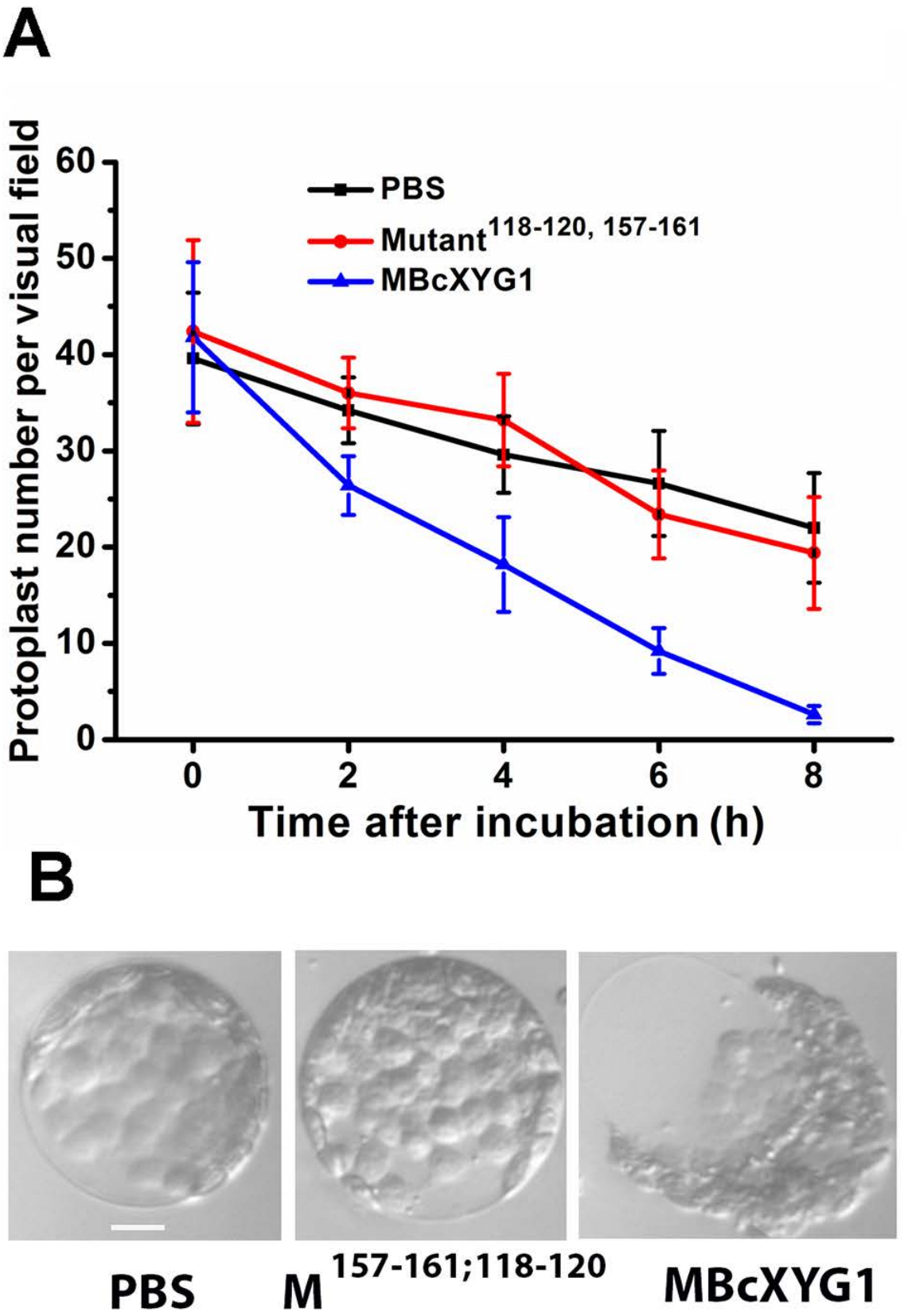

Figure 10 BcXYG1 triggers cell death on the plant cell membrane. *N. benthamiana* protoplasts were incubated with 100 μg/ml protein. A, The number of intact protoplasts was counted at the indicated time points. Data represent the means and standard deviations from three independent biological repeats with a total of 15 visual field for each treatment. B, Images of tobacco protoplasts 1 h after beginning of incubation. Bars = 10 μm.

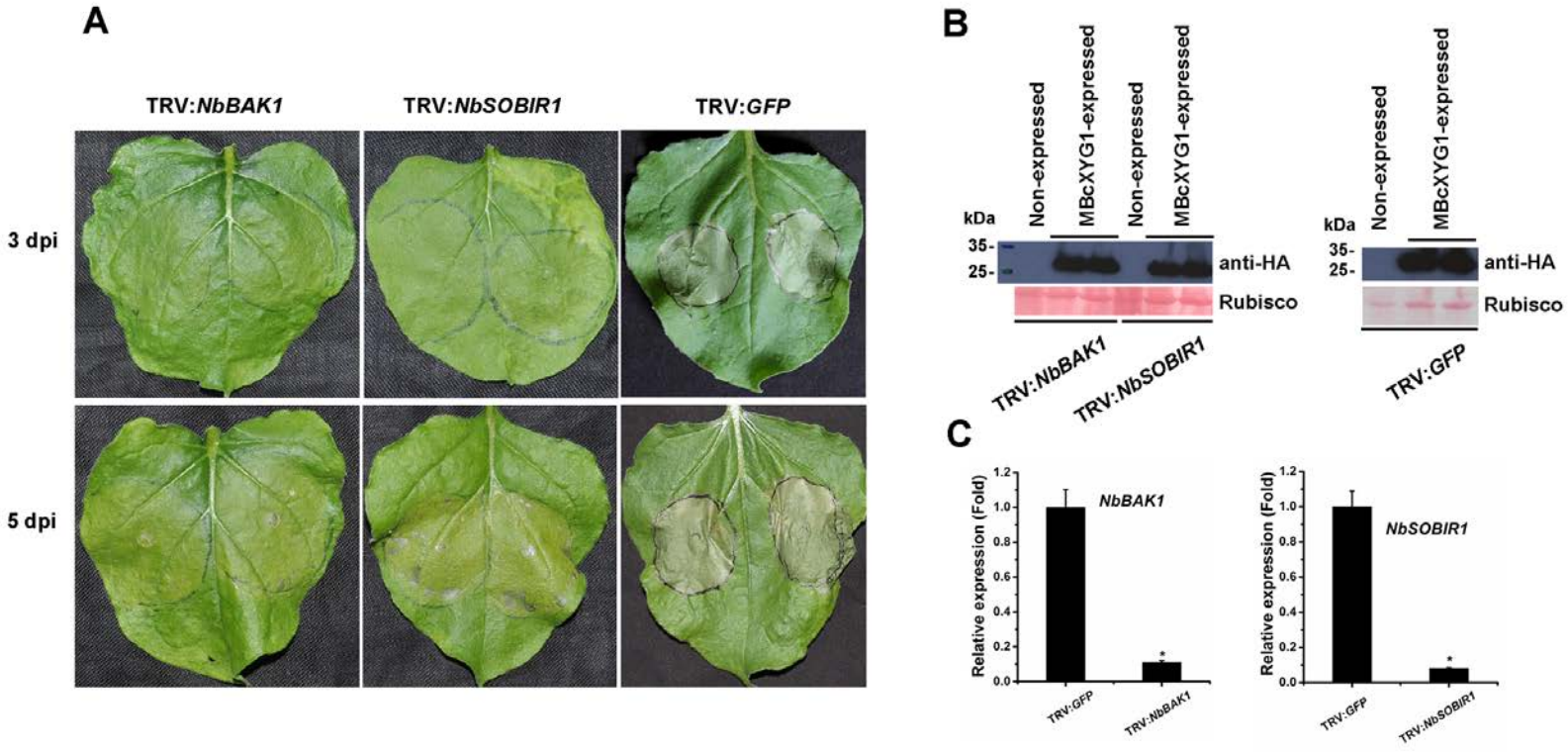

Figure 11 **Necrosis-inducing activity of BcXYG1 is mediated by *NbBAK1* and *NbSOBIR1*.** TRV-based VIGS vectors were used to initiate silencing of *NbBAK1* (TRV:*NbBAK1*) and *NbSOBIR1* (TRV:*NbSOBIR1*). TRV:*GFP* was used as a control virus treatment in these experiments. A, Three weeks after initiation of VIGS, *MBcXYG1* (+SP) was transiently expressed in the gene-silenced leaves using Agrobacterium infiltration. Leaves were photographed three and five days after treatment. B, Immunoblot analysis of proteins from indicated *N. benthamiana* leaves transiently expressing MBcXYG1-HA. Upper panel: MBcXYG1-HA was detected using anti-HA antibodies; lower panel: Ponceau S stained blots showing the Rubisco large subunit. C, Tobacco *NbBAK1* and *NbSOBIR1* expression levels after VIGS treatment determined by qRT-PCR analysis. Expression level in control plants (TRV:*GFP*) was set as 1. *NbEF1α* was used as an endogenous control. Means and standard deviations from three biological replicates are shown. Asterisks indicate significant differences (P = 0.01).

Parsed Citations

Albert I, Böhm H, Albert M, Feiler CE, Imkampe J, Wallmeroth N, Brancato C, Raaymakers TM, Oome S, Zhang H et al. (2015) An RLP23-SOBIR1-BAK1complex mediates NLP-triggered immunity. Nat Plants 1: 15140
Pubmed: Author and Title
CrossRef: Author and Title
Google Scholar: Author Only Title Only Author and Title

Benedetti M, Pontiggia D, Raggi S, Cheng Z, Scaloni F, Ferrari S, Ausubel FM, Cervone F, De Lorenzo G (2015) Plant immunity triggered by engineered in vivo release of oligogalacturonides, damage-associated molecular patterns. Proc Natl Acad Sci USA 112: 5533-5538
Pubmed: Author and Title
CrossRef: Author and Title
Google Scholar: Author Only Title Only Author and Title

Blanco-Ulate B, Morales-Cruz A, Amrine KCH, Labavitch JM, Powell ALT, Cantu D (2014) Genome-wide transcriptional profiling of Botrytis cinerea genes targeting plant cell walls during infections of different hosts. Front Plant Sci 5: 435.
Pubmed: Author and Title
CrossRef: Author and Title
Google Scholar: Author Only Title Only Author and Title

Böhm H, Albert I, Oome S, Raaymakers TM, Van den Ackerveken G, Nürnberger T (2014) A conserved peptide pattern from a widespread microbial virulence factor triggers pattern-induced immunity in Arabidopsis. PLoS Pathog 10: e1004491
Pubmed: Author and Title
CrossRef: Author and Title
Google Scholar: Author Only Title Only Author and Title

Brito N, Espino JJ, González C (2006) The endo-beta-1,4-xylanase xyn11A is required for virulence in Botrytis cinerea. Mol Plant Microbe Interact 19: 25-32
Pubmed: Author and Title
CrossRef: Author and Title
Google Scholar: Author Only Title Only Author and Title

Cantarel BL, Coutinho PM, Rancurel C, Bernard T, Lombard V, Henrissat B (2009) The carbohydrate-active enzymes database (CAZy): an expert resource for glycogenomics. Nucleic Acids Res 37: D233-D238
Pubmed: Author and Title
CrossRef: Author and Title
Google Scholar: Author Only Title Only Author and Title

Cheng Y, Wu K, Yao J, Li S, Wang X, Huang L, Kang Z (2016) PSTha5a23, a candidate effector from the obligate biotrophic pathogen Puccinia striiformis f. sp. tritici, is involved in plant defense suppression and rust pathogenicity. Environ Microbiol doi: 10.1111/1462-2920.13610. (Epub ahead of print).
Pubmed: Author and Title
CrossRef: Author and Title
Google Scholar: Author Only Title Only Author and Title

Cuesta Arenas Y, Kalkman ERIC, Schouten A, Dieho M, Vredenbregt P, Uwumukiza B, Osés Ruiz M, van Kan JAL (2010) Functional analysis and mode of action of phytotoxic Nep1-like proteins of Botrytis cinerea. Physiol Mol Plant Pathol 74: 376-386
Pubmed: Author and Title
CrossRef: Author and Title
Google Scholar: Author Only Title Only Author and Title

De Wit PJ (2016) Apoplastic fungal effectors in historic perspective; a personal view. New Phytol 212: 805-813
Pubmed: Author and Title
CrossRef: Author and Title
Google Scholar: Author Only Title Only Author and Title

Du J, Verzaux E, Chaparro-Garcia A, Bijsterbosch G, Keizer LC, Zhou J et al. (2015) Elicitin recognition confers enhanced resistance to Phytophthora infestans in potato. Nat Plants 1: 15034
Pubmed: Author and Title
CrossRef: Author and Title
Google Scholar: Author Only Title Only Author and Title

Du Y, Stegmann M, Misas Villamil JC (2016) The apoplast as battleground for plant-microbe interactions. New Phytol 209: 34-38
Pubmed: Author and Title
CrossRef: Author and Title
Google Scholar: Author Only Title Only Author and Title

Durrant WE, Dong X (2004) Systemic acquired resistance. Annu Rev Phytopathol 42: 185-209
Pubmed: Author and Title
CrossRef: Author and Title
Google Scholar: Author Only Title Only Author and Title

Eizner E, Ronen M, Gur Y, Gavish A, Zhu W, Sharon A (2017) Characterization of Botrytis-plant interactions using PathTrack© - an automated system for dynamic analysis of disease development. Mol Plant Pathol 18: 503-512
Pubmed: Author and Title
CrossRef: Author and Title
Google Scholar: Author Only Title Only Author and Title

El Oirdi M, El Rahman TA, Rigano L, El Hadrami A, Rodriguez MC, Daayf F, Vojnov A, Bouarab K (2011) Botrytis cinerea manipulates

the antagonistic effects between immune pathways to promote disease development in tomato. The Plant Cell 23: 2405-2421
Pubmed: Author and Title
CrossRef: Author and Title
Google Scholar: Author Only Title Only Author and Title

Espino JJ, Gutiérrez-Sánchez G, Brito N, Shah P, Orlando R, González C (2010) The Botrytis cinerea early secretome. Proteomics 10: 3020-3034
Pubmed: Author and Title
CrossRef: Author and Title
Google Scholar: Author Only Title Only Author and Title

Fang A, Han Y, Zhang N, Zhang M, Liu L, Li S, Lu F, Sun W (2016) Identification and characterization of plant cell death-inducing secreted proteins from Ustilaginoidea virens. Mol Plant Microbe Interact 29: 405-416
Pubmed: Author and Title
CrossRef: Author and Title
Google Scholar: Author Only Title Only Author and Title

Ferrari S, Plotnikova JM, Loren GD, Ausubel FM (2003) Arabidopsis local resistance to Botrytis cinerea involves salicylic acid and camalexin and requires EDS4 and PAD2, but not SID2, EDS5 or PAD4. The Plant J 35: 193-205
Pubmed: Author and Title
CrossRef: Author and Title
Google Scholar: Author Only Title Only Author and Title

Ferrari S, Savatin DV, Sicilia F, Gramegna G, Cervone F, De Lorenzo G (2013) Oligogalacturonides: plant damage-associated molecular patterns and regulators of growth and development. Front Plant Sci 4: 49
Pubmed: Author and Title
CrossRef: Author and Title
Google Scholar: Author Only Title Only Author and Title

Frías M, González M, González C, Brito N (2016) BcIEB1, a Botrytis cinerea secreted protein, elicits a defense response in plants. Plant Sci 250: 115-124
Pubmed: Author and Title
CrossRef: Author and Title
Google Scholar: Author Only Title Only Author and Title

Frías M, Brito N, González M, González C (2014) The phytotoxic activity of the cerato-platanin BcSpl1 resides in a two-peptide motif in the protein surface. Mol Plant Pathol 15: 342-351
Pubmed: Author and Title
CrossRef: Author and Title
Google Scholar: Author Only Title Only Author and Title

Frías M, Brito N, González C (2013) The Botrytis cinerea cerato-platanin BcSpl1 is a potent inducer of systemic acquired resistance (SAR) in tobacco and generates a wave of salicylic acid expanding from the site of application. Mol Plant Pathol 14:191-196
Pubmed: Author and Title
CrossRef: Author and Title
Google Scholar: Author Only Title Only Author and Title

Frías M, González C, Brito N (2011) BcSpl1, a cerato-platanin family protein, contributes to Botrytis cinerea virulence and elicits the hypersensitive response in the host. New Phytol 192: 483-495
Pubmed: Author and Title
CrossRef: Author and Title
Google Scholar: Author Only Title Only Author and Title

Furman-Matarasso N, Cohen E, Du Q, Chejanovsky N, Hanania U, Avni A (1999) A point mutation in the ethylene-inducing xylanase elicitor inhibits the beta-1-4-endoxylanase activity but not the elicitation activity. Plant Physiol 121: 345-351
Pubmed: Author and Title
CrossRef: Author and Title
Google Scholar: Author Only Title Only Author and Title

Franco-Orozco B, Berepiki A, Ruiz O, Gamble L, Griffe LL, Wang S, Birch PR, Kanyuka K, Avrova A (2017) A new proteinaceous pathogen-associated molecular pattern (PAMP) identified in Ascomycete fungi induces cell death in Solanaceae. New Phytol doi: 10.1111/nph.14542. [Epub ahead of print]
Pubmed: Author and Title
CrossRef: Author and Title
Google Scholar: Author Only Title Only Author and Title

Gao Y, Faris JD, Liu Z, Kim YM, Syme RA, Oliver RP, Xu SS, Friesen TL (2015) Identification and characterization of the SnTox6-Snn6 interaction in the Parastagonospora nodorum-wheat pathosystem. Mol Plant Microbe Interact 28: 615-625
Pubmed: Author and Title
CrossRef: Author and Title
Google Scholar: Author Only Title Only Author and Title

Glazebrook J (2005) Contrasting mechanisms of defense against biotrophic and necrotrophic pathogens. Annu Rev Phytopathol 43: 205-227
Pubmed: Author and Title
CrossRef: Author and Title
Google Scholar: Author Only Title Only Author and Title

González C, Brito N, Sharon A (2016) Botrytis-the fungus, the pathogen and its management in agricultural systems. Springer

International Publishing Switzerland 2016. Chapter 12: 229-246
Pubmed: Author and Title
CrossRef: Author and Title
Google Scholar: Author Only Title Only Author and Title

Grant M, Lamb C (2006) Systemic immunity. Curr Opin Plant Biol 9: 414-420
Pubmed: Author and Title
CrossRef: Author and Title
Google Scholar: Author Only Title Only Author and Title

Guo XM, Stotz HU (2007) Defense against Sclerotinia sclerotiorum in Arabidopsis is dependent on jasmonic acid, salicylic acid, and ethylene signaling. Mol Plant Microbe Interact 20: 1384-1395
Pubmed: Author and Title
CrossRef: Author and Title
Google Scholar: Author Only Title Only Author and Title

Kabbage M, Williams B, Dickman MB (2013) Cell death control: The interplay of apoptosis and autophagy in the pathogenicity of Sclerotinia sclerotiorum. PLoS Pathog 9: e1003287
Pubmed: Author and Title
CrossRef: Author and Title
Google Scholar: Author Only Title Only Author and Title

Kabbage M, Yarden O, Dickman MB (2015) Pathogenic attributes of Sclerotinia sclerotiorum: switching from a biotrophic to necrotrophic lifestyle. Plant Sci 233: 53-60
Pubmed: Author and Title
CrossRef: Author and Title
Google Scholar: Author Only Title Only Author and Title

Kettles GJ, Bayon C, Canning G, Rudd JJ, Kanyuka K (2017) Apoplastic recognition of multiple candidate effectors from the wheat pathogen Zymoseptoria tritici in the nonhost plant Nicotiana benthamiana. New Phytol 213: 338-350
Pubmed: Author and Title
CrossRef: Author and Title
Google Scholar: Author Only Title Only Author and Title

Koornneef A, Pieterse CMJ (2008) Cross talk in defense signaling. Plant Physiol 146: 839-844.
Pubmed: Author and Title
CrossRef: Author and Title
Google Scholar: Author Only Title Only Author and Title

Kubicek CP, Starr TL, Glass NL (2014) Plant cell wall-degrading enzymes and their secretion in plant-pathogenic fungi. Annu Rev Phytopathol 52: 427-451
Pubmed: Author and Title
CrossRef: Author and Title
Google Scholar: Author Only Title Only Author and Title

Liebrand TW, van den Berg GC, Zhang Z, Smit P, Cordewener JH, America AH, Sklenar J, Jones AM, Tameling WI, Robatzek S, Thomma BP, Joosten MH (2013) Receptor-like kinase SOBIR1/EVR interacts with receptor-like proteins in plant immunity against fungal infection. Proc Natl Acad Sci USA 110: 10010-10015
Pubmed: Author and Title
CrossRef: Author and Title
Google Scholar: Author Only Title Only Author and Title

Lorang J, Kidarsa T, Bradford CS, Gilbert B, Curtis M, Tzeng SC, Maier CS, Wolpert TJ (2012) Tricking the guard: exploiting plant defense for disease susceptibility. Science 338: 659-662
Pubmed: Author and Title
CrossRef: Author and Title
Google Scholar: Author Only Title Only Author and Title

Lorang JM, Sweat TA, Wolpert TJ (2007) Plant disease susceptibility conferred by a "resistance" gene. Proc Natl Acad Sci USA 104: 14861-14866
Pubmed: Author and Title
CrossRef: Author and Title
Google Scholar: Author Only Title Only Author and Title

Ma L, Salas O, Bowler K, Oren-Young L, Bar-Peled M, Sharon A (2017a) Genetic alteration of UDP-rhamnose metabolism in Botrytis cinerea leads to accumulation of UDP-KDG that adversely affects development and pathogenicity. Mol Plant Pathol 18: 263-275
Pubmed: Author and Title
CrossRef: Author and Title
Google Scholar: Author Only Title Only Author and Title

Ma Z, Song T, Zhu L, Ye W, Wang Y, Shao Y, Dong S, Zhang Z, Dou D, Zheng X, Tyler BM, Wang Y (2015) A Phytophthora sojae glycoside hydrolase 12 protein is a major virulence factor during soybean infection and is recognized as a PAMP. Plant Cell 27: 2057-2072
Pubmed: Author and Title
CrossRef: Author and Title
Google Scholar: Author Only Title Only Author and Title

Ma Z, Zhu L, Song T, Wang Y, Zhang Q, Xia Y, Qiu M, Lin Y, Li H, Kong L, Fang Y, Ye W, Wang Y, Dong S, Zheng X, Tyler BM, Wang Y (2017b) A paralogous decoy protects Phytophthora sojae apoplastic effector PsXEG1 from a host inhibitor. Science 355: 710-714

Pubmed: Author and Title
CrossRef: Author and Title
Google Scholar: Author Only Title Only Author and Title

Marianayagam NJ, Sunde M, Matthews JM (2004) The power of two: protein dimerization in biology. Trends Biochem Sci 29: 618-625
Pubmed: Author and Title
CrossRef: Author and Title
Google Scholar: Author Only Title Only Author and Title

Master ER, Zheng Y, Storms R, Tsang A, Powlowski J (2008) A xyloglucan-specific family 12 glycosyl hydrolase from Aspergillus niger: recombinant expression, purification and characterization. Biochem J 411: 161-170
Pubmed: Author and Title
CrossRef: Author and Title
Google Scholar: Author Only Title Only Author and Title

Minz-Dub A, Kokkelink L, Tudzynski B, Tudzynski P, Sharon A (2013) Involvement of Botrytis cinerea small GTPases BcRAS1 and BcRAC in differentiation, virulence and the cell cycle. Eukaryot Cell 12: 1609-1618
Pubmed: Author and Title
CrossRef: Author and Title
Google Scholar: Author Only Title Only Author and Title

Mur LAJ, Kenton P, Atzorn R, Miersch O, Wasternack C (2006) The outcomes of concentration-specific interactions between salicylate and jasmonate signaling include synergy, antagonism, and oxidative stress leading to cell death. Plant Physiol 140: 249-262
Pubmed: Author and Title
CrossRef: Author and Title
Google Scholar: Author Only Title Only Author and Title

Nesvizhskii AI, Keller A, Kolker E, Aebersold R (2003) A statistical model for identifying proteins by tandem mass spectrometry. Anal Chem 75:4646-4658
Pubmed: Author and Title
CrossRef: Author and Title
Google Scholar: Author Only Title Only Author and Title

Noda J, Brito N, González C (2010) The Botrytis cinerea xylanase Xyn11A contributes to virulence with its necrotizing activity, not with its catalytic activity. BMC Plant Biol 10: 38
Pubmed: Author and Title
CrossRef: Author and Title
Google Scholar: Author Only Title Only Author and Title

Oliver RP, Friesen TL, Faris JD, Solomon PS (2012) Stagonospora nodorum: from pathology to genomics and host resistance. Annu Rev Phytopathol 50: 23-43
Pubmed: Author and Title
CrossRef: Author and Title
Google Scholar: Author Only Title Only Author and Title

Oome S, Raaymakers TM, Cabral A, Samwel S, Böhm H, Albert I, Nürnberger T, Van den Ackerveken G (2014) Nep1-like proteins from three kingdoms of life act as a microbe-associated molecular pattern in Arabidopsis. Proc Natl Acad Sci USA 111: 16955-16960
Pubmed: Author and Title
CrossRef: Author and Title
Google Scholar: Author Only Title Only Author and Title

Oliver RP, Solomon PS (2010) New developments in pathogenicity and virulence of necrotrophs. Curr Opin Plant Biol 13: 415-419
Pubmed: Author and Title
CrossRef: Author and Title
Google Scholar: Author Only Title Only Author and Title

Ottmann C, Luberacki B, Küfner I, Koch W, Brunner F et al. (2009) A common toxin fold mediates microbial attack and plant defense. Proc Natl Acad Sci USA 106: 10359-10364
Pubmed: Author and Title
CrossRef: Author and Title
Google Scholar: Author Only Title Only Author and Title

Pétriacq P, Stassen JH, Ton J (2016) Spore density determines infection strategy by the plant pathogenic fungus Plectosphaerella cucumerina. Plant Physiol 170: 2325-2339
Pubmed: Author and Title
CrossRef: Author and Title
Google Scholar: Author Only Title Only Author and Title

Poinssot B, Vandelle E, Bentéjac M, Adrian M, Levis C, Brygoo Y, Garin J, Sicilia F, Coutos-Thévenot P, Pugin A (2003) The endopolygalacturonases 1 from Botrytis cinerea activates grapevine defense reactions unrelated to its enzymatic activity. Mol Plant Microbe Interact 16: 553-564
Pubmed: Author and Title
CrossRef: Author and Title
Google Scholar: Author Only Title Only Author and Title

Postma J, Liebrand TWH, Bi G, Evrard A, Bye RR, Mbengue M, Kuhn H, Joosten MHAJ, Robatzek S (2016) Avr4 promotes Cf-4 receptor-like protein association with the BAK1/SERK3 receptor-like kinase to initiate receptor endocytosis and plant immunity. New Phytol 210: 627-642

Pubmed: Author and Title
CrossRef: Author and Title
Google Scholar: Author Only Title Only Author and Title

Rossi FR, Gárriz A, Marina M, Romero FM, Gonzalez ME, Collado IG, Pieckenstain FL (2011) The sesquiterpene botrydial produced by Botrytis cinerea induces the hypersensitive response on plant tissues and its action is modulated by salicylic acid and jasmonic acid signaling. Mol Plant Microbe Interact 24: 888-896
Pubmed: Author and Title
CrossRef: Author and Title
Google Scholar: Author Only Title Only Author and Title

Sandgren M, Shaw A, Ropp TH, Wu S, Bott R, Cameron AD, Ståhlberg J, Mitchinson C, Jones TA (2001) The X-ray crystal structure of the Trichoderma reesei family 12 endoglucanase 3, Cel12A, at 1.9 A resolution. J Mol Biol 308: 295-310
Pubmed: Author and Title
CrossRef: Author and Title
Google Scholar: Author Only Title Only Author and Title

Sandgren M, Ståhlberg J, Mitchinson C (2005) Structural and biochemical studies of GH family 12 cellulases: improved thermal stability, and ligand complexes. Prog Biophys Mol Bio 89: 246-291
Pubmed: Author and Title
CrossRef: Author and Title
Google Scholar: Author Only Title Only Author and Title

Segmüller N, Kokkelink L, Giesbert S, Odinius D, van Kan J, Tudzynski P (2008) NADPH oxidases are involved in differentiation and pathogenicity in Botrytis cinerea. Mol Plant Microbe Interact 21: 808-819
Pubmed: Author and Title
CrossRef: Author and Title
Google Scholar: Author Only Title Only Author and Title

Sevier CS, Kaiser CA (2002) Formation and transfer of disulphide bonds in living cells. Nat Rev Mol Cell Bio 3: 836-847
Pubmed: Author and Title
CrossRef: Author and Title
Google Scholar: Author Only Title Only Author and Title

Shalit T, Elinger D, Savidor A, Gabashvili A, Levin Y (2015) MS1-based label-free proteomics using a quadrupole orbitrap mass spectrometer. J Proteome Res 14: 1979-1986
Pubmed: Author and Title
CrossRef: Author and Title
Google Scholar: Author Only Title Only Author and Title

Shi G, Friesen TL, Saini J, Xu SS, Rasmussen JB, Faris JD (2015) The wheat Snn7 gene confers susceptibility on recognition of the Parastagonospora nodorum necrotrophic effector SnTox7. The Plant Genome 8: 1-10
Pubmed: Author and Title
CrossRef: Author and Title
Google Scholar: Author Only Title Only Author and Title

Shlezinger N, Minz A, Gur Y, Hatam I, Dagdas YF et al. (2011) Anti-apoptotic machinery protects the necrotrophic fungus Botrytis cinerea from host-induced apoptotic-like cell death during plant infection. PLoS Pathog 7: e1002185
Pubmed: Author and Title
CrossRef: Author and Title
Google Scholar: Author Only Title Only Author and Title

Spoel SH, Johnson JS, Dong X (2007) Regulation of tradeoffs between plant defenses against pathogens with different lifestyles. Proc Natl Acad Sci USA 104: 18842-18847
Pubmed: Author and Title
CrossRef: Author and Title
Google Scholar: Author Only Title Only Author and Title

Trouvelot S, Héloir MC, Poinssot B, Gauthier A, Paris F, Guillier C et al. (2014) Carbohydrates in plant immunity and plant protection: roles and potential application as foliar sprays. Front Plant Sci 5: 592
Pubmed: Author and Title
CrossRef: Author and Title
Google Scholar: Author Only Title Only Author and Title

van Kan JAL, Shaw MW, Grant-Downton RT (2014) Botrytis species: relentless necrotrophic thugs or endophytes gone rogue? Mol Plant Pathol 15: 957-961
Pubmed: Author and Title
CrossRef: Author and Title
Google Scholar: Author Only Title Only Author and Title

Wei W, Zhu W, Cheng J, Xie J, Jiang D, Li G, Chen W, Fu Y (2016) Nox complex signal and MAPK cascade pathway are cross-linked and essential for pathogenicity and conidiation of mycoparasite Coniothyrium minitans. Sci Rep 6: 24325
Pubmed: Author and Title
CrossRef: Author and Title
Google Scholar: Author Only Title Only Author and Title

Williams B, Kabbage M, Kim HJ, Britt R, Dickman MB (2011) Tipping the balance: Sclerotinia sclerotiorum secreted oxalic acid suppresses host defenses by manipulating the host redox environment. PLoS Pathog 7: e1002107
Pubmed: Author and Title
CrossRef: Author and Title
Google Scholar: Author Only Title Only Author and Title

Williamson B, Tudzynski B, Tudzynski P, van Kan JA (2007) Botrytis cinerea: the cause of grey mould disease. Mol Plant Pathol 8: 561-580
Pubmed: Author and Title
CrossRef: Author and Title
Google Scholar: Author Only Title Only Author and Title

Wu J, Wang Y, Park SY, Kim SG, Yoo JS, Park S, Gupta R, Kang KY, Kim ST (2016) Secreted alpha-N-arabinofuranosidase B protein is required for the full virulence of Magnaporthe oryzae and triggers host defences. PLoS ONE 11: e0165149
Pubmed: Author and Title
CrossRef: Author and Title
Google Scholar: Author Only Title Only Author and Title

Xiang J, Li X, Yin L, Liu Y, Zhang Y, Qu J, Lu J (2017) A candidate RxLR effector from Plasmopara viticola can elicit immune responses in Nicotiana benthamiana. BMC Plant Biol 17: 75
Pubmed: Author and Title
CrossRef: Author and Title
Google Scholar: Author Only Title Only Author and Title

Zhang H, Wu Q, Cao S, Zhao T, Chen L, Zhuang P, Zhou X, Gao Z (2014a) A novel protein elicitor (SsCut) from Sclerotinia sclerotiorum induces multiple defense responses in plants. Plant Mol Biol 86: 495-511
Pubmed: Author and Title
CrossRef: Author and Title
Google Scholar: Author Only Title Only Author and Title

Zhang L, Kars I, Essenstam B, Liebrand TW, Wagemakers L, Elberse J et al. (2014b) Fungal endopolygalacturonases are recognized as microbe-associated molecular patterns by the Arabidopsis receptor-like protein RESPONSIVENESS TO BOTRYTIS POLYGALACTURONASES1. Plant Physiol 164: 352-364
Pubmed: Author and Title
CrossRef: Author and Title
Google Scholar: Author Only Title Only Author and Title

Zhang L, Ni H, Du X, Wang S, Ma XW, Nürnberger T, Guo HS, Hua C (2017) The Verticillium-specific protein VdSCP7 localizes to the plant nucleus and modulates immunity to fungal infections. New Phytol doi: 10.1111/nph.14537. [Epub ahead of print]
Pubmed: Author and Title
CrossRef: Author and Title
Google Scholar: Author Only Title Only Author and Title

Zhang W, Fraiture M, Kolb D, Loffelhardt B, Desaki Y, Boutrot FF et al. (2013) Arabidopsis receptor-like protein 30 and receptor-like kinase suppressor of BIR1-1/EVERSHED mediate innate immunity to necrotrophic fungi. Plant Cell 25: 4227-4241
Pubmed: Author and Title
CrossRef: Author and Title
Google Scholar: Author Only Title Only Author and Title

Zhang Y, Zhang Y, Qiu D, Zeng H, Guo L, Yang X (2015) BcGs1, a glycoprotein from Botrytis cinerea, elicits defence response and improves disease resistance in host plants. Biochem Bioph Res Co 457: 627-634
Pubmed: Author and Title
CrossRef: Author and Title
Google Scholar: Author Only Title Only Author and Title

Zhu W, Wei W, Fu Y, Cheng J, Xie J, Li G, Yi X, Kang Z, Dickman MB, Jiang D (2013) A secretory protein of necrotrophic fungus Sclerotinia sclerotiorum that suppresses host resistance. PLoS ONE 8: e53901
Pubmed: Author and Title
CrossRef: Author and Title
Google Scholar: Author Only Title Only Author and Title